Investigating the metabolic changes that accompany skeletal muscle hypertrophy

by

Linnea Rimmer

B.S., Kansas State University, 2021

A THESIS

Submitted in partial fulfillment of the requirements for the degree

MASTER OF SCIENCE

Department of Animal Sciences and Industry
College of Agriculture

KANSAS STATE UNIVERSITY
Manhattan, Kansas

2023

Approved by:

Major Professor
Morgan Daughtry Zumbaugh

Copyright

Abstract

The meat industry must increase production output with fewer agricultural inputs to sustain the growing global population. Innovative strategies to improve feed efficiency in swine can reduce production expenses and feed requirements. Skeletal muscle is responsible for up to 90% of all glucose use in meat producing animals, and therefore has become a target to improve nutrient utilization efficiency. For example, an increase in muscle oxidative capacity is associated with lower feed efficiency in pigs. To define the metabolic changes in skeletal muscle that accompany maturation, samples were collected from the *longissimus dorsi* (LD, glycolytic muscle), *latissimus dorsi* (LAT, mixed muscle), and *masseter* (MS, oxidative muscle) at 20, 53, 87, 120, and 180 days of age from DNA 600 x 241 (DNA Genetics) castrated male pigs that weighed an average of 5.7, 20.8, 42.2, 83.4, and 130.5 kg, respectively. Ages correspond to the end of each phase diet typical of those fed in commercial production, which are formulated to meet nutrient requirements to support each period of growth. Muscles were assessed to determine the abundance of several metabolic enzymes through Western blotting. Additionally, mitochondria were isolated and incubated with [$^{13}C_3$]-pyruvate in an *in vitro* tracing model to analyze isotopomer enrichment patterns of tricarboxylic acid cycle (TCA) intermediates to investigate how mitochondria metabolize pyruvate. Glucose-6-phosphate dehydrogenase decreased at 87, 120, and 180 d in MS compared to LAT and LD ($P < 0.01$), which suggests glycolytic muscles increase intermediate allocation to the pentose phosphate pathway at this time whereas oxidative muscles do not. Moreover, pyruvate carboxylase (PC) increased at 53 d compared to 20, 87, 120, and 180 d ($P < 0.01$), while pyruvate dehydrogenase increased at 120 d compared to 53 d ($P < 0.05$) indicating there was a shift in pyruvate entry into the TCA cycle. Oxaloacetate M3 mole percent excess and

citrate synthase increased at 120 d ($P < 0.01$), while citrate M3 mole percent excess decreased at 120 d ($P < 0.01$). These data suggest pyruvate-derived citrate exits the TCA cycle at 120 d by an unidentified cataplerotic reaction. Additionally, alpha-ketoglutarate M3 mole percent excess increased at 180 d in LD and LAT compared to MS ($P < 0.01$), and abundance of glutamate dehydrogenase increased at 180 d ($P < 0.05$), which indicates a portion of pyruvate-derived carbons could be exiting the TCA cycle at 180 d through glutamate dehydrogenase. These findings have established a metabolic fingerprint associated with muscle hypertrophy and provides the framework to uncover the regulatory mechanism that modulates nutrient allocation to major metabolic pathways in growing muscle. Elucidating this mechanism will aid in providing innovative strategies to improve feed efficiency in the swine industry.

Table of Contents

List of Figures

List of Abbreviations

CSA	Cross sectional area
ETC	Electron transport chain
FE	Feed efficiency
FOXO3	Forkhead box 03
G6P	Glucose-6-phosphate
G6PDH	Glucose-6-phosphate dehydrogenase
GDH	Glutamate dehydrogenase
GLUT4	Glucose transporter type 4
GOT2	Glutamic-oxaloacetic transaminase 2
IGF-1	Insulin-like growth factor-1
LAT	Latissimus dorsi
LD	Longissimus dorsi
LDHα	Lactate dehydrogenase alpha
MS	Masseter
MTBSTFA	N-tert-Butyldimethylsiyl-N-methyltrifluoroacetamide
mtDNA	Mitochondrial DNA
mTOR	mammalian target of rapamycin
mTORC1	mammalian target of rapamycin complex 1
NADPH	Nicotinamide adenine dinucleotide phosphate
PBS	Phosphate buffer saline
PC	Pyruvate carboxylase
PDH	Pyruvate dehydrogenase
PI3K	Phosphatidylionositol-3 kinase
PIP2	Phosphatidylinositol-4-5-bisphosphate
PIP3	Phosphatidylinositol-3,4,5-trisphophate
PDK1	Phosphoinositide-dependent kinase 1
PPP	Pentose phosphate pathway
SREBPs	Sterol regulatory element binding proteins
tBDMS	Tertiary-butyldimethylsilyl
TCA	Tricarboxylic acid

Acknowledgements

Dr. Morgan Zumbaugh: I do not know where to begin with my thanks to you. I would not have been given this incredible opportunity without your reaching hand. You have pushed me to be the better scientist that I am today, and I am beyond grateful for everything you have taught me. These past two years have been some of the hardest times in my life, but you were always there for me and helped me get through it. I am looking forward to our future and I am excited for the new journey I am about to embark on with you. Thank you for being an amazing professor, advisor, mentor and friend.

Dr. Michael Chao: Thank you for all of the encouragement and support you have given me even before starting the program. Most importantly, thank you for continuously answering my questions, troubleshooting protocols and encouraging me to go out of the box to come up with solutions. Thank you for being on my committee, and I am looking forward to continue working with you throughout my PhD program.

Dr. Tavis O'Quinn: Thank you for taking the time to teach me about statistics and applied meat science. I came in knowing very little about meat science, but being a TA for your ASI 350 course helped me tremendously. I am forever grateful for that experience. Thank you for being on my committee, and I look forward to learning more from you throughout my PhD program and hopefully become a statistics wizard like you.

Dr. Erika Geisbrecht: Thank you for always taking the time to answer any questions that I had regarding biochemical reactions and cellular processes. It was a pleasure working with you and I thank you for being on my committee.

Dr. Jason Woodworth: Thank you for helping me with the live swine part of my study and providing additional information to help me understand my project better. Thank you for always being willing to assist with my project. I greatly appreciate all of your help.

Dr. Charles Arthur Zumbaugh III: Thank you for our weekly meetings and teaching me the ways of R Studio. Although it took a while for me to get the hand of the program, you always pushed me to continue with it. I am forever grateful for having your mentorship.

Meat Science Graduate Students: I am enormously appreciative for each and every graduate student who has been involved with my project. From cutting muscle samples with tiny scissors to encouraging me on the hard days to celebrating victories on good days, I will never forget the times we had. Most importantly, I am grateful for all of the friendships that I have made throughout my program and I am looking forward to cherishing many more.

Brittany Smith and Chanae Parker: Thank you for your hard work and dedication towards my project. I am so thankful that I was able to work with you two and teach you the ins and outs of the lab. You both are going to make amazing scientists.

My family: Thank you for all the love, support, encouragement, advise you provided. You may have not known what I was talking about at times, but you always provided positive feedback. I want to give a special thanks to my parents: **Drew and Erika Rimmer**. I love you both so much. You have always supported my education, no matter what direction I went. In fact, you encouraged me to follow my dreams and apply for graduate school. **Annika and Erik Rimmer**: Thank you for being the best siblings and celebrating the small wins with me. **Da, Papa, MorMor and FarFar**: Thank you for being the best grandparents a girl can ask for. You're endless support does not go unnoticed. I love you all very much.

Grace Corrette: Thank you for all of your support, guidance, and encouragement throughout our program. Although we bonded through the hardship of biochemistry, I am forever grateful that our program brought us together and now we are best friends. I will cherish our friendship for life.

Alexis Fenton: Thank you for being there for it all. The good and stressful times. The times where we either celebrated or blew off some steam. I am beyond grateful to have you as my best friend and the world's best roommate.

Carson Funk: Thank you for the endless love and support. Even long-distance you were always there for me and continuously encouraging me that I can do anything that I set my mind to. I cannot thank you enough nor show you how much I appreciate you. I love you so much.

Dedication

I would like to dedicate this thesis to my mother Erika Rimmer. I am heartbroken we could not share these past six months together, but we will celebrate sometime soon. You were the one who encouraged me to take a leap of faith and join the meat science department, and I am so glad that I took your advice. I love you.

Chapter 1 - Literature Review

Introduction

The global population is projected to reach nearly nine billion people by 2050 (Tripathi, 2019), which compromises the amount of arable land available to sustain this rate of population growth (Zahid et al., 2016). Therefore, innovative approaches are necessary to produce more food with less resources to feed our growing population. While all agricultural products face this challenge, an increase in global wealth permits additional meat consumption in populations that were once limited to plant-based diets. As such, the livestock industry must increase production by 38% from 2020 to 2050 to accommodate more meat-eaters and an increase in population (Komarek et al., 2021). To date, scientists have utilized growth promotants, feed additives, improved nutrition, and genetic selection to increase meat-animal production (Wu et al., 2011; Khanal et al., 2019). Although successful and essential for continued improvements, innovative strategies are necessary to further improve production efficiency with less resources. Understanding the biochemical mechanisms that regulate nutrient utilization in major metabolic pathways of skeletal muscle in meat producing animals holds great potential to improve feed efficiency (FE).

Skeletal muscle accounts for 40-50% of body weight and is responsible for up to 80% of an animal's glucose use (Guo, 2019; Merz and Thurmond, 2021). Skeletal muscle cells utilize nutrients to produce ATP or conversely as building blocks in anabolic processes that facilitate muscle growth. Although the former is necessary under certain physiological circumstances, the latter is a requisite for efficient lean deposition. For example, complete oxidation of nutrients results in ATP, CO_2, heat, and water, which results in a net loss of carbon by the animal. On the other hand, glycolytic metabolism can conserve carbon backbones to support the synthesis of

amino acids or fatty acids. However, the mechanism that dictates nutrient allocation in skeletal muscle of livestock species remains elusive. Therefore, this literature review aims to give an overview of the major metabolic pathways in muscle and discuss the implications of different metabolic characteristics on the efficiency of substrate utilization.

Implications of Skeletal Muscle Metabolism on Production Efficiency

Skeletal muscle is a dynamic tissue that responds to extrinsic and intrinsic stimuli. Although several aspects of muscle physiology are plastic, changes in muscle metabolism have implications on the efficiency of an animal's nutrient utilization, and thus FE. Skeletal muscle metabolism is a set of complex biochemical pathways that are orchestrated by a variety of signaling events in response to changing stimuli (de Lange et al., 2007). For example, activity level, nutrition, environmental conditions, species, and genetics influence muscle metabolism (Picard et al., 2002; Buzala et al., 2015; Niyas et al., 2015). These factors dictate the degree to which muscle relies on glycolysis or oxidative phosphorylation. The dynamic interplay between these two major metabolic pathways allows muscle to adjust its metabolic profile and gives rise to a heterogenous population of muscle fibers, which can be classified by metabolism (oxidative or glycolytic) and contractile speed (slow or fast). While slow fibers (type I) rely heavily on oxidative metabolism, presumably to fuel long or continuous bouts of work, fast fibers (type IIa, IIx, and IIb) vary in their metabolic capability and can range from having a high oxidative capacity to a high glycolytic capacity. In fact, mitochondrial content ranges from approximately 5 – 25 percent of total fiber volume in type II fibers (Mishra et al., 2015). For example, type IIb fibers are on the lower end of the range of mitochondrial content and have a high abundance of glycolytic enzymes (Schiaffino and Reggiani, 2011). On the other hand, type IIa fibers have a high abundance of mitochondria and oxidative enzymes. The heterogeneity of muscle results in a wide range of metabolic

characteristics and plays a vital role in how nutrient such as amino acids, carbohydrates, and fatty acids are utilized to meet the animal's needs (Frontera and Ochala, 2015).

The degree to which cells rely on glycolysis or oxidative phosphorylation influences FE of pigs. For example, muscle in pigs with high FE exhibit lower abundance of oxidative enzymes than those with low FE (Fu et al., 2017). Further, ractopamine supplementation increases protein accretion, which is attributed to several factors including nutrient repartitioning from adipose tissue to muscle and a metabolic shift to increase glycolytic metabolism in muscle (Halsey et al., 2011; James et al., 2013a; Costa-Lima et al., 2015). Commercial diets, which are subject to continuous optimization for FE, also influence muscle metabolic characteristics. High carbohydrate and energy dense diets result in an increased glycolytic metabolism (Cline et al., 2022), and in fact, muscle mitochondrial networks are quite responsive to nutrient changes. For example, isolated type IIX/B single muscle fibers cultured *ex vivo* in high glucose media exhibit punctate mitochondria whereas those in media containing acetate and no glucose form extensive networks after an overnight incubation (Mishra et al., 2015). Amino acid profile in swine diets also impact metabolic enzyme expression in muscle. Pigs supplemented with excess methionine for 2 weeks before slaughter increases lactate dehydrogenase and decreases citrate synthase (CS) abundance in muscle (Gondret et al., 2021), which are respective glycolytic and oxidative enzymes. These findings depict the dynamic nature of muscle and highlight an area of muscle physiology that can be exploited to aid in the effort to improve FE of livestock, although the underlying mechanism that facilitates these changes remains unclear.

Glycolysis

Glycolysis converts glucose to pyruvate through a series of stepwise enzymatic reactions in the sarcoplasm of muscle cells. During periods of nutrient surplus, such as those after feeding,

glucose is taken up by muscle cells through glucose transporter type 4 (GLUT4) and rapidly converted to glucose-6-phosphate (G6P) by hexokinase to permit additional glucose uptake. During short bouts of nutrient scarcity, such as those between feedings, myofibers metabolize glycogen reserves to generate glucose-1-phosphate, which is converted to G6P to continue to supply glycolytic intermediates to generate ATP. At this stage, G6P can continue through glycolysis or branch off into the pentose phosphate pathway (PPP). Entry into this anabolic pathway is catabolized by glucose-6-phosphate dehydrogenase (G6PDH) and produces 5-carbon precursors for nucleic acid and amino acid synthesis. In fact, mammalian target of rapamycin complex 1 (mTORC1) activation of sterol regulatory element binding proteins (SREBPs) increases flux through the PPP, which provides nicotinamide adenine dinucleotide phosphate (NADPH) and carbon-rich precursors for nucleotide synthesis associated with muscle hypertrophy (Liu and Sabatini, 2020).

However, the bulk of G6P will continue to be metabolized through subsequent glycolytic reactions to generate pyruvate, which can enter the Cori Cycle or the tricarboxylic acid (TCA) cycle depending on cellular needs. In the Cori Cycle, lactate dehydrogenase alpha (LDHα) converts pyruvate to lactate that is exported from muscle and shuttled to the liver for gluconeogenesis. Greater abundance of LDHα and reliance on the Cori Cycle occurs predominately in glycolytic muscle. In fact, it has been reported that there is an increase in LDHα and an improved FE in pigs fed ractopamine (James et al., 2013a, b). On the other hand, pyruvate can be oxidized fully in the TCA cycle to produce ATP during periods of high energy demand or oxidized partially for use as a precursor for biosynthetic reactions.

Tricarboxylic Acid Cycle

The TCA cycle is a series of enzymatic reactions that catabolize pyruvate, amino acids, and fatty acids to generate reducing equivalents that are oxidized in the electron transport chain (ETC) to produce ATP. The TCA cycle is not a carbon sink, and as such, entry and exit of intermediates from the TCA cycle are coupled. Anaplerotic enzymes are those that result in an influx of intermediates, such as pyruvate dehydrogenase (PDH) or pyruvate carboxylase (PC) that facilitate pyruvate entering the TCA cycle. The former results in acetyl-CoA and CO_2, which represents a net loss of carbon by the animal, whereas the latter consumes HCO_3^- to produce oxaloacetate. Although the majority of pyruvate anaplerosis occurs through PDH, PC mediated entry does not expel CO_2 and is necessary under certain circumstances. During periods of high acetyl-CoA levels, such as during a fed state, pyruvate entry shifts from PDH to PC because acetyl-CoA is a positive allosteric regulator of PC (Shi and Tu, 2015). Oxaloacetate produced from PC can be used in the TCA cycle or converted to malate to exit mitochondria through for fatty acid synthesis (White et al., 2019). In fact, muscle in high FE pigs exhibit a higher abundance of PC than low FE pigs (Fu et al., 2017).

For continued anaplerosis, an efflux of intermediates termed cataplerosis is required. For example, glutamic-oxaloacetic transaminase 2 (GOT2) is a cataplerotic enzyme that converts oxaloacetate to aspartate through transamination. Aspartate is shuttled out of mitochondria through the glutamate-aspartate antiporter where it can be converted to glutamate, which can be used to synthesis other amino acids or be catabolized to produce ATP (Cruzat and Tirapegul, 2015). Glutamate dehydrogenase (GDH) catalyzes a reversible reaction that converts α-ketoglutarate to glutamate, consumes NH_4^+, and oxidizes NADPH to $NADP^+$ when acting as a cataplerotic enzyme. Conversely, glutamate anaplerosis generates NH_4^+ and NADPH, which is used in other

biosynthetic reactions including fatty acid synthesis. (Plaitakis et al., 2017). The TCA cycle has long been depicted as a robust and all-consuming catabolic pathway; however, these dynamic enzymes are orchestrated by intermediate flux, which is changing continuously depending on cellular energy status.

Electron Transport Chain

Reducing equivalents generated in glycolysis or the TCA cycle are oxidized to produce ATP by the ETC (Balaban, 1990), which consists of five complexes in the inner membrane of mitochondria. These are complex I (NADH-ubiquinone oxidoreductase), complex II (succinate:ubiquinone oxidoreductase), complex III (ubiquinol-cytochrome *c* reductase), complex IV (cytochrome *c* oxidase), and complex V (ATP synthase). Two electron carriers shuttle electrons from complex I/II to III and from complex III to IV termed ubiquinone and cytochrome *c*, respectively. To generate the membrane potential that powers mitochondria, complex I and II oxidize NADH and $FADH_2$ to produce NAD^+ and FADH. These oxidized electron carriers are then reduced in glycolysis or the TCA cycle to continue to facilitate these processes. Cytochrome c shuttles electrons to complex IV where oxygen is reduced to H_2O. Additionally, complexes I, III, and IV pump protons across the inner membrane to generate the mitochondrial membrane potential. The majority of protons re-enter the matrix through ATP synthase (complex V), which harnesses this energy to synthesize ATP from ADP and inorganic phosphate (Frazier, 2011; Tabassum, 2020). This is termed coupled respiration or ATP-linked respiration, whereas protons that re-enter the matrix through an alternative route is termed uncoupled respiration.

During uncoupled respiration, protons do not flow through complex V but rather cross the membrane through membrane uncoupling proteins (UCPs) or by non-specific transmembrane flux, termed mitochondrial proton leak. Leaks can occur from a variety of sources and are primarily

activated by fatty acids, superoxide, or peroxidation products (Jastroch et al., 2010). Uncoupled respiration is necessary under certain physiological conditions, such as through the nicotinamide nucleotide transhydrogenase that reduces $NADP^+$ to NADPH to combat reactive oxygen species in the glutathione and thioredoxin pathways. However, mitochondrial proton leak may be a source of mitochondrial inefficiency that has negative implications on FE. Indeed, broilers with high FE have a greater glutamate-stimulated respiratory control ratio than low FE broilers (Bottje et al., 2002), which is indicative of coupled respiration. In another example, low residual feed intake steers have a greater glutamate- and succinate- stimulated respiratory control ratio than high residual feed intake steers (Kolath et al., 2006). These data demonstrate changes in mitochondrial respiration also have implications on FE in broilers and cattle.

Skeletal muscle growth

Nutrient distribution to different tissues in a growing animal change from birth to maturity and can be divided into four phases. After birth, phase I is characterized by growth and nutrient allocation to vital organs, bone development, visceral fat and the nervous system. The next phase of growth allocates nutrients to support rapid muscle growth whereas the last two phases end muscle growth and increase fat deposition (Gerrard and Grant, 2003). To optimize FE, the swine industry utilizes a programmed feeding schedule that is based on tissue specific energy needs throughout a pig's life (Tokach et al., 2016), and commercial swine diets are formulated to support these phases of growth. For example, essential amino acids and high quality ingredients are fed in the first phase, whereas carbohydrates are primarily fed in the final growth phases for optimal lean muscle growth and fat laydown (Tokach et al., 2016). The last phase requires significant energy to deposit fat. In fact, it takes four times the amount of energy to deposit one pound of fat compared to a pound of muscle (Schumacher et al., 2022). Therefore, understanding the physiological

changes that facilitate porcine growth is imperative to continue to improvement feed conversion in commercial swine operations.

Skeletal muscle growth is a delicate balance of anabolic and catabolic reactions that support muscle hypertrophy (Glass, 2005). The insulin-like growth factor-1 (IGF-1) / phosphatidylionositol-3 kinase (PI3K) / Akt signaling pathway and myostatin pathway are two major regulatory pathways that promote and inhibit protein accretion, respectively (Stitt et al., 2004; Glass, 2005). Binding of IGF-1 to its receptor stimulates the activation of PI3K, which phosphorylates phosphatidylinositol-4-5-bisphosphate (PIP2) to phosphatidylinositol-3,4,5-trisphophate (PIP3) to create a lipid binding site for phosphoinositide-dependent kinase 1 (PDK1) to activate Akt. Many downstream targets are regulated by Akt including several regulatory targets for protein synthesis, such as mammalian target of rapamycin (mTOR). In fact, muscle lacking mTOR exhibit severe metabolic dysregulation and a myopathy that mimics muscular dystrophy (Risson et al., 2009). Further, activation of Akt inhibits phosphorylation of forkhead box O3 (FOXO3) protein to inhibit proteolysis and stimulates protein synthesis through the activation of mTOR (Zhao et al., 2007). Stimulation of IGF-1 results in protein synthesis through activation of the PI3K-Akt pathway, whereas inactivation of IGF-1 and the overexpression of FOXO3 induces muscle atrophy (Zhao et al., 2007). Further, overexpression of IGF-1 in muscle results in a higher rate of glucose disposal and higher respiratory quotient (volume of carbon dioxide released over the volume of oxygen absorbed), which suggests carbohydrates are the preferred nutrient source in IGF-1 mediated hypertrophy (Christoffolete et al., 2015). Indeed, GLUT4 abundance increased 2-fold and a shift from type IIA to type IIB occurred in extensor digitorum longus muscles overexpressing IGF-1 (Christoffolete et al., 2015). These data demonstrate IGF-1 activity in muscle provokes metabolic changes within muscle as well as impacts global glucose disposal.

Further, nutrient intake influences circulating IGF-1 levels, which can also impact muscle characteristics. For example, circulating IGF-1 levels are greater in lambs with low residual feed than lambs with high residual feed intake (Montelli et al., 2021). These findings highlight the underlying metabolic changes that accompany hypertrophic signaling in muscle.

Myostatin, a negative regulator of skeletal muscle growth, is an important mediator of catabolic pathways and is essential for cell homeostasis (Carnac et al., 2007). Since the PI3K/Akt cascade is found in both IGF-1 and myostatin signaling, cross-communication between these pathways regulates normal muscle growth by balancing muscle atrophy and hypertrophy. Overexpression of myostatin decreases muscle hypertrophy through downregulation of the mTOR pathway (Amirouche et al., 2009), whereas myostatin deficiency increases rates of protein synthesis and skeletal muscle hypertrophy (Lipina et al., 2010). In addition to being a potent regulator of muscle mass, myostatin also has implications on muscle metabolism. For example, hypertrophy in muscle lacking myostatin is accompanied by a decrease in oxidative capacity and a shift towards a glycolytic phenotype (Mouisel et al., 2014). In normal muscle physiology, myostatin plays a delicate role in modulating muscle mass and seemingly plays a role in muscle metabolism, although it is unclear if myostatin is a direct mediator of metabolism or an adaptation to support the extensive hypertrophy. Overall, the interplay between these muscle mass regulatory pathways has implications on hypertrophy and the underlying metabolic characteristics of muscle.

Summary

Skeletal muscle is a dynamic tissue that is responsive to external and internal stimuli. Therefore, production practices ranging from genetics to environmental stressors influence muscle physiology, which have implications on an animal's growth performance. As outlined in this chapter, conditions that provoke greater bouts of hypertrophy are associated with a shift towards

glycolytic metabolism. Although it is unclear what underlying mechanism facilitates a shift in metabolism, it is apparent that glycolysis can generate ATP while conserving carbon backbones to be used in anabolic pathways. For example, glycolytic intermediates can branch into the PPP to generate 5-carbon precursors for nucleotide synthesis or its final product, pyruvate, can be converted to lactate in the Cori cycle. On the other hand, oxidative metabolism has the capacity to generate more ATP per mole of pyruvate and is necessary in certain physiological conditions but generates CO_2, heat, and H_2O, which represents an area of inefficiency to the animal in converting nutrients to muscle. However, mitochondrial metabolism is more complex in nature than simply acting as a cellular furnace. In fact, TCA intermediates can exit at several points in the cycle through cataplerotic reactions (Martinez-Reyes and Chandel, 2020), which plays an important role in several biosynthetic processes. Therefore, a deeper understanding of how muscle coordinates these metabolic pathways to facilitate hypertrophy will aid in the effort to improve the efficiency of lean deposition in meat producing animals.

References

Amirouche, A., A. C. Durieux, S. Banzet, N. Koulmann, R. Bonnefoy, C. Mouret, X. Bigard, A. Peinnequin, and D. Freyssenet. 2009. Down-regulation of Akt/mammalian target of rapamycin signaling pathway in response to myostatin overexpression in skeletal muscle. Endocrinology 150(1):286-294. doi: 10.1210/en.2008-0959

Balaban, R. S. 1990. Regulation of oxidative phosphorylation in the mammalian cell. Am J Physiol 258(3 Pt 1):C377-389. doi: 10.1152/ajpcell.1990.258.3.C377

Bottje, W., M. Iqbal, Z. X. Tang, D. Cawthon, R. Okimoto, T. Wing, and M. Cooper. 2002. Association of mitochondrial function with feed efficiency within a single genetic line of male broilers. Poult Sci 81(4):546-555. doi: 10.1093/ps/81.4.546

Buzala, M., B. Janicki, and R. Czarnecki. 2015. Consequences of different growth rates in broiler breeder and layer hens on embryogenesis, metabolism and metabolic rate: A review. Poult Sci 94(4):728-733. doi: 10.3382/ps/pev015

Carnac, G., B. Vernus, and A. Bonnieu. 2007. Myostatin in the pathophysiology of skeletal muscle. Curr Genomics 8(7):415-422. doi: 10.2174/138920207783591672

Christoffolete, M. A., W. J. Silva, G. V. Ramos, M. R. Bento, M. O. Costa, M. O. Ribeiro, M. M. Okamoto, T. H. Lohmann, U. F. Machado, A. Musaro, and A. S. Moriscot. 2015. Muscle IGF-1-induced skeletal muscle hypertrophy evokes higher insulin sensitivity and carbohydrate use as preferential energy substrate. Biomed Res Int 2015:282984. doi: 10.1155/2015/282984

Cline, P. M., T. C. Tsai, C. A. Lents, A. M. Stelzleni, C. R. Dove, and M. Azain. 2022. Interaction of dietary carbohydrate and fat on glucose metabolism in growing pigs. Domest Anim Endocrinol 78:106655. doi: 10.1016/j.domaniend.2021.106655

Costa-Lima, B. R., S. P. Suman, S. Li, C. M. Beach, T. J. Silva, E. T. Silveira, B. M. Bohrer, and D. D. Boler. 2015. Dietary ractopamine influences sarcoplasmic proteome profile of pork Longissimus thoracis. Meat Sci 103:7-12. doi: 10.1016/j.meatsci.2014.12.008

Cruzat, V. F., and J. Tirapegul. 2015. Glutamine in Clinical Nutrition. Springer.

de Lange, P., M. Moreno, E. Silvestri, A. Lombardi, F. Goglia, and A. Lanni. 2007. Fuel economy in food-deprived skeletal muscle: signaling pathways and regulatory mechanisms. FASEB J 21(13):3431-3441. doi: 10.1096/fj.07-8527rev

El-Kadi, S. W., R. L. t. Baldwin, K. R. McLeod, N. E. Sunny, and B. J. Bequette. 2009. Glutamate is the major anaplerotic substrate in the tricarboxylic acid cycle of isolated rumen epithelial and duodenal mucosal cells from beef cattle. J Nutr 139(5):869-875. doi: 10.3945/jn.108.103226

Frazier, A. E., Thorburn, David R. 2011. Biochemical Analyses of the Electron Transport Chain Complexes by Spectrophotometry, Mitochondrial Disorders No. 837. p. 49-62.

Frontera, W. R., and J. Ochala. 2015. Skeletal muscle: a brief review of structure and function. Calcif Tissue Int 96(3):183-195. doi: 10.1007/s00223-014-9915-y

Fu, L., Y. Xu, Y. Hou, X. Qi, L. Zhou, H. Liu, Y. Luan, L. Jing, Y. Miao, S. Zhao, H. Liu, and X. Li. 2017. Proteomic analysis indicates that mitochondrial energy metabolism in skeletal muscle tissue is negatively correlated with feed efficiency in pigs. Sci Rep 7:45291. doi: 10.1038/srep45291

Gerrard, D., and A. Grant. 2003. Principles of Animal Growth and Development. Kendall/Hunt Publishing Company.

Glass, D. J. 2005. Skeletal muscle hypertrophy and atrophy signaling pathways. Int J Biochem Cell Biol 37(10):1974-1984. doi: 10.1016/j.biocel.2005.04.018

Gondret, F., N. Le Floc'h, D. I. Batonon-Alavo, M. H. Perruchot, Y. Mercier, and B. Lebret. 2021. Flash dietary methionine supply over growth requirements in pigs: Multi-facetted effects on skeletal muscle metabolism. Animal 15(7):100268. doi: 10.1016/j.animal.2021.100268

Guo, X., Zhang, W., Li, M., Gao, P., He, Z., Wu, Y., Cai, C., Li, B., Cao., G. 2019. Transcriptome profile of skeletal muscle at different developmental stages in Large White and Mashen pigs. Canadian Journal of Animal Science 99. doi: 10.1139/cjas-2019-0002

Halsey, C. H., P. S. Weber, S. S. Reiter, B. N. Stronach, J. L. Bartosh, and W. G. Bergen. 2011. The effect of ractopamine hydrochloride on gene expression in adipose tissues of finishing pigs. J Anim Sci 89(4):1011-1019. doi: 10.2527/jas.2010-3269

James, B. W., M. D. Tokach, R. D. Goodband, J. L. Nelssen, S. S. Dritz, K. Q. Owen, J. C. Woodworth, and R. C. Sulabo. 2013a. Effects of dietary L-carnitine and ractopamine HCl on the metabolic response to handling in finishing pigs. J Anim Sci 91(9):4426-4439. doi: 10.2527/jas.2011-4411

James, B. W., M. D. Tokach, R. D. Goodband, J. L. Nelssen, S. S. Dritz, K. Q. Owen, J. C. Woodworth, and R. C. Sulabo. 2013b. Interactive effects of dietary ractopamine HCl and L-carnitine on finishing pigs: I. Growth performance. J Anim Sci 91(7):3265-3271. doi: 10.2527/jas.2011-4286

Jastroch, M., A. S. Divakaruni, S. Mookerjee, J. R. Treberg, and M. D. Brand. 2010. Mitochondrial proton and electron leaks. Essays Biochem 47:53-67. doi: 10.1042/bse0470053

Khanal, P., C. Maltecca, C. Schwab, K. Gray, and F. Tiezzi. 2019. Genetic parameters of meat quality, carcass composition, and growth traits in commercial swine. J Anim Sci 97(9):3669-3683. doi: 10.1093/jas/skz247

Kolath, W. H., M. S. Kerley, J. W. Golden, and D. H. Keisler. 2006. The relationship between mitochondrial function and residual feed intake in Angus steers. J Anim Sci 84(4):861-865. doi: 10.2527/2006.844861x

Komarek, A. M., S. Dunston, D. Enahoro, H. C. J. Godfray, M. Herrero, D. Mason-D'Croz, K. M. Rich, P. Scarborough, M. Springmann, T. B. Sulser, K. Wiebe, and D. Willenbockel. 2021. Income, consumer preferences, and the future of livestock-derived food demand. Glob Environ Change 70:102343. doi: 10.1016/j.gloenvcha.2021.102343

Lipina, C., H. Kendall, A. C. McPherron, P. M. Taylor, and H. S. Hundal. 2010. Mechanisms involved in the enhancement of mammalian target of rapamycin signalling and hypertrophy in skeletal muscle of myostatin-deficient mice. FEBS Lett 584(11):2403-2408. doi: 10.1016/j.febslet.2010.04.039

Liu, G. Y., and D. M. Sabatini. 2020. mTOR at the nexus of nutrition, growth, ageing and disease. Nat Rev Mol Cell Biol 21(4):183-203. doi: 10.1038/s41580-019-0199-y

Martinez-Reyes, I., and N. S. Chandel. 2020. Mitochondrial TCA cycle metabolites control physiology and disease. Nat Commun 11(1):102. doi: 10.1038/s41467-019-13668-3

Matarneh, S. K., C. N. Yen, J. Bodmer, S. W. El-Kadi, and D. E. Gerrard. 2021. Mitochondria influence glycolytic and tricarboxylic acid cycle metabolism under postmortem simulating conditions. Meat Sci 172:108316. doi: 10.1016/j.meatsci.2020.108316

Merz, K. E., and D. C. Thurmond. 2021. Role of Skeletal Muscle in Insulin Resistance and Glucose Uptake. Comparative Physiology 10(3)doi: 10.1002/cphy.c190029

Mishra, P., G. Varuzhanyan, A. H. Pham, and D. C. Chan. 2015. Mitochondrial Dynamics is a Distinguishing Feature of Skeletal Muscle Fiber Types and Regulates Organellar Compartmentalization. Cell Metab 22(6):1033-1044. doi: 10.1016/j.cmet.2015.09.027

Montelli, N., T. Alvarenga, A. K. Almeida, F. A. P. Alvarenga, I. F. Furusho-Garcia, P. L. Greenwood, and I. G. Pereira. 2021. Associations of feed efficiency with circulating IGF-1 and leptin, carcass traits and meat quality of lambs. Meat Sci 173:108379. doi: 10.1016/j.meatsci.2020.108379

Mouisel, E., K. Relizani, L. Mille-Hamard, R. Denis, C. Hourde, O. Agbulut, K. Patel, L. Arandel, S. Morales-Gonzalez, A. Vignaud, L. Garcia, A. Ferry, S. Luquet, V. Billat, R. Ventura-Clapier, M. Schuelke, and H. Amthor. 2014. Myostatin is a key mediator between energy metabolism and endurance capacity of skeletal muscle. Am J Physiol Regul Integr Comp Physiol 307(4):R444-454. doi: 10.1152/ajpregu.00377.2013

Niyas, A., C. K, S. S, S. V, B. R, B. M, Rao, Kurien, and Girish. 2015. Adaptation of Livestock to Environmental Challenges. doi: 10.4172/2325-9590.1000146

Picard, B., L. Lefaucheur, C. Berri, and M. J. Duclos. 2002. Muscle fibre ontogenesis in farm animal species. Reprod Nutr Dev 42(5):415-431. doi: 10.1051/rnd:2002035

Plaitakis, A., E. Kalef-Ezra, D. Kotzamani, I. Zaganas, and C. Spanaki. 2017. The Glutamate Dehydrogenase Pathway and Its Roles in Cell and Tissue Biology in Health and Disease. Biology (Basel) 6(1)doi: 10.3390/biology6010011

Risson, V., L. Mazelin, M. Roceri, H. Sanchez, V. Moncollin, C. Corneloup, H. Richard-Bulteau, A. Vignaud, D. Baas, A. Defour, D. Freyssenet, J. F. Tanti, Y. Le-Marchand-Brustel, B. Ferrier, A. Conjard-Duplany, K. Romanino, S. Bauche, D. Hantai, M. Mueller, S. C. Kozma, G. Thomas, M. A. Ruegg, A. Ferry, M. Pende, X. Bigard, N. Koulmann, L. Schaeffer, and Y. G. Gangloff. 2009. Muscle inactivation of mTOR causes metabolic and dystrophin defects leading to severe myopathy. J Cell Biol 187(6):859-874. doi: 10.1083/jcb.200903131

Scheffler, T. L., J. M. Scheffler, S. Park, S. C. Kasten, Y. Wu, R. P. McMillan, M. W. Hulver, M. I. Frisard, and D. E. Gerrard. 2014. Fiber hypertrophy and increased oxidative capacity can occur simultaneously in pig glycolytic skeletal muscle. Am J Physiol Cell Physiol 306(4):C354-363. doi: 10.1152/ajpcell.00002.2013

Schiaffino, S., and C. Reggiani. 2011. Fiber types in mammalian skeletal muscles. Physiol Rev 91(4):1447-1531. doi: 10.1152/physrev.00031.2010

Schumacher, M., H. DelCurto-Wyffels, J. Thomson, and J. Boles. 2022. Fat Deposition and Fat Effects on Meat Quality-A Review. Animals (Basel) 12(12)doi: 10.3390/ani12121550

Shi, L., and B. P. Tu. 2015. Acetyl-CoA and the regulation of metabolism: mechanisms and consequences. Curr Opin Cell Biol 33:125-131. doi: 10.1016/j.ceb.2015.02.003

Stitt, T. N., D. Drujan, B. A. Clarke, F. Panaro, Y. Timofeyva, W. O. Kline, M. Gonzalez, G. D. Yancopoulos, and D. J. Glass. 2004. The IGF-1/PI3K/Akt pathway prevents expression of muscle atrophy-induced ubiquitin ligases by inhibiting FOXO transcription factors. Mol Cell 14(3):395-403. doi: 10.1016/s1097-2765(04)00211-4

Tabassum, N., Kheya, Ilora Shabnam, Asaduzzaman, Syed Abdullah Ibn, Maniha, Syeda Muntaka, Fayz, Abrar Hamim, Zakaria, Amayna, Noor, Rashed. 2020. A Review on the Possible Leakage of Electrons through the Electron Transport Chain within Mitochondria. Biomedical Research and Environmental Sciences 1(4)doi: 10.37871/jels1127

Tokach, M. D., B. D. Goodband, and T. G. O'Quinn. 2016. Performance-enhancing technologies in swine production. doi: doi.org/10.2527/af.2016-0039

Tripathi, A. D., Mishra, Richa, Maurya, Kamlesh K., Singh, Ram B., Wilson, Douglas W. 2019. Estimates for World Population and Global Food Availability for Global Health. In: R. B. Singg, Watson, Ronald Ross, Takahashi, Toru, editor, The Role of Functional Food Security in Global Health. p. 3-24.

White, B. A., J. R. Harrison, and L. M. Mehlmann. 2019. Energy Metabolism. Endocrine and Reproductive Physiology 3:40-76.

Wu, G., F. W. Bazer, G. A. Johnson, D. A. Knabe, R. C. Burghardt, T. E. Spencer, X. L. Li, and J. J. Wang. 2011. Triennial Growth Symposium: important roles for L-glutamine in swine nutrition and production. J Anim Sci 89(7):2017-2030. doi: 10.2527/jas.2010-3614

Zahid, H. J., E. Robinson, and R. L. Kelly. 2016. Agriculture, population growth, and statistical analysis of the radiocarbon record. Proc Natl Acad Sci U S A 113(4):931-935. doi: 10.1073/pnas.1517650112

Zhao, J., J. J. Brault, A. Schild, P. Cao, M. Sandri, S. Schiaffino, S. H. Lecker, and A. L. Goldberg. 2007. FoxO3 coordinately activates protein degradation by the autophagic/lysosomal and proteasomal pathways in atrophying muscle cells. Cell Metab 6(6):472-483. doi: 10.1016/j.cmet.2007.11.004

Chapter 2 - Investigating the metabolic changes that accompany skeletal muscle maturation

Introduction

Scientists predict global livestock production must increase 38% from 2020 to 2050 to satisfy the growing demand for meat (Komarek et al., 2021). Since the 1950s, continuous advancements in genetics, nutrition, and precision agriculture have revolutionized animal production. In the US swine industry today, market pigs require 4% less feed and have a 17% heavier carcass than those reared three decades ago (Tokach et al., 2016). While traditional production strategies are unarguably imperative for continued advancements, additional improvements are becoming more difficult to obtain. For example, feed conversion ratios decreased 26% on feeder-to-finish operations from 1992 to 2004 but only decreased 3% from 2004 to 2009 (McBride and Key, 2013), which is presumably a result of exhausting the current technologies and strategies to improve feed conversion ratios. Feed production and transportation represent the largest environmental impact and financial burden associated with pork production (Patience et al., 2015; Andretta et al., 2021). Therefore, innovative strategies to further improve feed efficiency (FE) are imperative to increase pork production with the growing constraints on agricultural land from population growth and urbanization.

Skeletal muscle accounts for 40-50% of body mass and is responsible for up to 80% of an animal's glucose use (Guo, 2019; Merz and Thurmond, 2021), and thus has significant impacts on feed utilization given swine diets are carbohydrate-based. Muscle is composed of a heterogenous population of muscle fibers that are classified by contractile speed (slow-twitch or fast-twitch) and metabolism (glycolytic or oxidative). Slow-twitch muscle fibers rely on oxidative metabolism,

while fast-twitch can range from highly oxidative to highly glycolytic (Julien et al., 2018). These metabolic characteristics influence nutrient utilization efficiency. For example, muscle in pigs with high FE exhibit a lower abundance of oxidative enzymes than those with low FE (Fu et al., 2017). It is apparent the degree to which muscle fibers rely on glycolysis or oxidative phosphorylation influences efficiency of lean growth; however, metabolic changes that accompany porcine muscle growth remain undefined.

Nutrient distribution to tissues in a growing animal change from birth to maturity and can be divided into four phases. After birth, phase I is characterized by growth and nutrient allocation to vital organs, bone development, and the nervous system. The next phase of growth allocates nutrients to support rapid muscle growth, whereas the last two phases end muscle growth and increase fat deposition (Gerrard and Grant, 2003). These distinct tissue growth phases explain why intensive feeding during finishing does not facilitate greater lean deposition but rather increases fat deposition (Bikker et al., 1994; Wagner et al., 1999). The last two phases of growth represent the biological ceiling for lean deposition, and as such, extending days to market results in fatter, not heavier, muscled carcasses. Further, the last phase requires about 4 times the amount of energy to deposit a pound of fat compared to a pound of muscle (Schumacher et al., 2022). To account for these vastly different nutritional needs, commercial swine operations use feeding programs that are developed to provide optimal nutrients associated with each growth phase (Tokach et al., 2016), which demonstrates the need to understand the physiological changes that control nutrient allocation and use to support lean accretion. Therefore, the objective of this study is to investigate the metabolic changes that accompany skeletal muscle hypertrophy.

Materials and Methods

Animal Harvest and Sample Collection

The protocol used in this experiment was approved by the Kansas State University Institutional Animal Care and Use Committee. The study utilized castrated male pigs (DNA 600 x 241; DNA Genetics, Columbus, NE) that were housed at the Kansas State University Swine Teaching and Research Center in Manhattan, KS. Pigs were provided *ab libitum* access to feed and water with each pen containing a single, dry self-feeder and nipple waterer. Prior to harvest, pigs consumed corn-soybean meal-based diets typical of those fed in commercial production that were formulated to meet or exceed the National Research Council (2012) estimates for nutrient requirement for pigs of the given weight range. In order to meet the nutrient requirements for these growing pigs, phase-feeding was implemented to ensure optimal growth. At 20, 53, 87, 120, and 180 days of age, pigs were transported to the KSU Meat Lab and harvested. Samples from the *longissimus dorsi* (LD), *latissimus dorsi* (LAT), and *masseter* (MS) were collected within fifteen minutes after exsanguination. Samples were divided and snap frozen in liquid nitrogen, frozen for histology, or used to isolate mitochondria. Samples snap frozen in liquid nitrogen were stored at -80°C until further analysis. Histology samples were submerged in plastic molds containing Optimal Cutting Media (Fisher Scientific, Hampton, NH), frozen in liquid nitrogen cooled isopentane, and stored at -80ºC. Mitochondria were immediately isolated for metabolite tracing.

Backfat Measurement

Backfat thickness (BF) was measured using a Renco Lean-Meater Digital Backfat Indicator (Renco Corporation, Golden Valley, MN). Five barrows of corresponding ages (25 d, 58 d, 92 d, 130 d, and 180 d) were ultrasonically measured for backfat. To determine the correct location for the BF measurement, the last rib was found and an oil spot 65 mm below the spine was marked.

Each barrow was measured twice, one measurement for each side of the loin and averaged together.

Histochemistry

Five-micron thick sections were cut using a 550 HM microm (ThermoFisher Scientific, Waltham, MA) and placed on saline coated slides. Slides were submerged in 1% hematoxylin (Fisher Scientific, Hampton, NH) for 3 min and rinsed in running deionized water. Slides were submerged in 50% eosin (Fisher Scientific, Hampton, NH) for 1 sec and rinsed with deionized water. Slides were submerged in increasing concentrations of ethanol, rinsed in xylene for 7 sec, dried with a Kimwipe (Kimberly-Clark Professional Kimtech Science, Fisher Scientific, Hampton, NH) and mounted with Epredia™ Shandon-Mount (Fisher Scientific, Hampton, NH). Images were taken with a Nikon Eclipse Ti2 inverted microscope (Nikon, Melville, NY) and analyzed with Nikon-Elements software.

Mitochondria Isolation

Mitochondria were isolated using the differential centrifugation method as described by Scheffler et al. (2014) and Matarneh et al. (2021) with minor modifications. Briefly, muscles were finely minced with scissors at 1.5:10 (wt/vol) in ice-cold homogenization buffer (pH 7.4) containing 100 mM sucrose, 180 mM KCl, 50 mM Tris, 5 mM $MgCl_2$, 10 mM EDTA, and 1 mM K-ATP. Protease from *Bacillus licheniformis* (Sigma Aldrich, St. Louis, MO) was added to the tissue suspension at a final concentration of 5 mg/ml and homogenized using a Potter-Elvehjem tissue homogenizer system (Glas-Col, Terre Haute, IN. USA). Homogenates were diluted with homogenization buffer to ~40 ml/g of tissue and filtered through cheesecloth. Filtered homogenates were centrifuged at 2,000 × g for 10 min, and supernatants were filtered again through cheesecloth. Filtered supernatants were centrifuged at 8000 × g for 10 min. Mitochondrial

pellets were resuspended in a modified KHEB buffer (pH 7.2) containing 120 mM KCl, 0.2 mM KH_2PO_4, 1 mM HEPES, and 0.5 mM EGTA. Mitochondrial protein concentration was determined by Thermo Scientific™ Pierce™ BCA Protein Assay Kit (Pierce, Rockford, IL) according to the manufacturer's instructions.

***In vitro* Metabolism Model**

In a microcentrifuge tube, 3 mg of mitochondria were added to 1 mL KHEB containing 1 mM malic acid, 5 mM ADP, and 1 mM sodium pyruvate-$^{13}C_3$ (Sigma Aldrich, St. Louis, MO). Unlabeled control reactions contained 1 mM sodium pyruvate. After incubation at 37°C on a rocker at 40 rpm for 45 min incubation, samples were mixed with 2 M perchloric acid, incubated on ice for 15 min, and centrifuged at 12,000 x g for 5 min. The supernatant was immediately transferred to new tubes, neutralized with 3 M KOH, and stored at -80°C until further analysis (Bergmeyer, 1984; Matarneh et al., 2021).

Mass Spectrometry of TCA metabolites

Samples and TCA intermediate standards were prepared for gas chromatography-mass spectrometry (GM-MS) using the deproteinization and derivatization method described by Metarneh et al. (2021). Briefly, 5 M hydroxylamine hydrochloride was added to the samples followed by the addition of 4 M KOH. At a basic pH, samples were sonicated and then acidified with 6 N HCl. Ethyl acetate was added to samples to extract the organic phase of the supernatant after centrifugation. Samples were evaporated to dryness under compressed N_2 at 40°C. Once dried, equal amounts of N-tert-Butyldimethylsilyl-N-methyltrifluoroacetamide (MTBSTFA) and ethyl acetate were added to form the tertiary-butyldimethylsilyl (tBDMS) derivatives during a 1 hr incubation period at 65°C. Samples were separated using gas chromatography (Agilent 6890N; Agilent, Santa Clara, CA, USA) on a J&W HP-5ms GC Column (HP-5MS, 30 m, 0.25 mm, 0.25

μm film; Agilent Technologies) as previously described by El-Kadi et al. (2009) with minor modifications. Intermediate ions with mass-to-charge (*m/z*) were evaluated using the single ion monitoring method with a mass spectrophotometer (Agilent 5973N; Agilent, Santa Clara, CA, USA). Ions monitored included: pyruvate 274.10, succinate 289.10, fumarate 287.10, malate 419.20, oxaloacetate 432.10, α-ketoglutarate 446.20, and citrate 591.40. Mole percent excess (MPE) are calculated as (M + i / M + 0) * 100, where M+ i is defined as the isotopic enrichment of a molecule.

Western Blotting

Muscle samples were pulverized in liquid nitrogen, homogenized in ice-cold IntactProtein™ lysis buffer (GenuIN Biotech, Blacksburg, VA) according to manufacturer's instructions, and centrifuged at 13,000 x g for 10 min at 4°C. Supernatants were collected and protein concentration was determined with a BCA Protein Assay Kit as mentioned previously. Samples were diluted in 2X laemmli sample buffer containing 2-mercaptoethanol, sodium dodecyl sulfate, glycerol, tris-chloride, bromophenol blue, and protease inhibitor mini tablets (Cat #. PIA32955, Fisher Scientific, Hampton, NH). Equal amounts of protein were separated using SDS-PAGE and transferred to PVDF or nitrocellulose membranes. Membranes were blocked with OneBlock blocking buffer (Prometheus Protein Biology Products, Genesee Scientific, San Diego, CA) and incubated with the corresponding primary antibody overnight at 4°C. Antibodies used for Western blot analysis include anti-LDHα (Cat #: NBPI-48336SS, Novus Biologicals, Centennial, CO), anti-GDH (Cat #: PIPA569381, Fisher Scientific, Hampton, NH), anti-G6PDH (Cat# NBPI-89805, Novus Biologicals, Centennial, CO), anti-GOT2 (Cat# NBP2-32241, Novus Biologicals, Centennial, CO), anti-PDHA1 (Cat# AV48137, Sigma Aldrich, St. Louis, MO), anti-CS (Cat# TA308265, OriGene, Rockville, MD), and anti-PC (Cat# NBPI-49536SS). Secondary antibodies

used include Goat anti-Rabbit IgG (H+L) Highly Cross-Adsorbed Secondary Antibody, Alexa Fluor™ Plus 647, Invitrogen™ (Cat# PIA32733, Fisher Scientific, Hampton, NH), and Goat anti-rabbit IgG antibody (H+L) HRP conjugate (Cat# AP307P, Sigma Aldrich, St. Louis, MO). Total protein abundance was measured with Invitrogen ™ No-Stain™ Protein labeling reagent (ThemroFisher Scientific, Walham, MA) following the manufacturer's instructions. Prior to imaging, ProSignal Pico ECL reagent (Prometheus Protein Biology, Genesee Scientific, San Diego, CA) was added to the membranes imaged with chemiluminescence for 45 sec and then drained. Membranes were imaged with the IBright Imaging System (ThermoFisher Scientific, Waltham, MA). Images were analyzed using Thermo Fisher iBright Analysis Software and normalized to the total protein abundance.

Real-Time PCR

Muscle samples were pulverized in liquid nitrogen, and DNA was extracted using Zymo Research Quick-DNA™ Miniprep Plus Kit following the manufacturer's solid tissue protocol (Zymo Research, Irvine, CA, USA). Concentration of DNA was determined with a Biotek Take3 Micro-Volume Plate (Agilent Technologies, Santa Clara, CA) using the Biotek Gen5 software. Primers from Lopez-Andreo et al. (2005), Taqman™ Fast Advanced Master Mix (Thermo Fisher, Waltham, MA), and MGB Applied Biosystems probes were used with sequences described in Table 1. QuantStudio3 Real-Time PCR system (ThermoFisher Scientific, Waltham, MA, USA) was used to carry out the qPCR reaction. Quantification was performed using the ΔΔCT method.

Oligonucleotide	**Sequence (5' to 3')**
Porcine mitochondrial *t-Glu* gene forward primer	GAA AAA TCA TCG TTG TAC TTC AAC TAC A
Porcine mitochondrial *cyt* B gene reverse primer	GGT CAA TGA ATG CGT TGT TGA T
Consensus eukaryotic 18S RNA gene nuclear forward primer	AGC CTG CGG CTT AAT TTG AC

Consensus eukaryotic 18S RNA gene nuclear reverse primer	CAA CTA AGA ACG GCC ATG CA
Consensus porcine *cyt* B gene mitochondrial probe	CCA CCC ACT AAT AAA
Consensus eukaryotic 18S RNA gene nuclear probe	AGG ATT GAC AGA TTGA G

Statistics section

Data were analyzed using a mixed effects model with fixed effects of muscle, age, and their interaction, and a random effect of pig. Data were considered significant when $P \leq 0.05$ and means were separated by pairwise comparisons using Tukey's HSD. Data are presented as the least squares means +/- standard error. All data were analyzed using R (version 4.2.1, Indianapolis, IN). Western blot data were log transformed to normalize the residuals. Data are presented as the back-transformed values.

Results and Discussion

Postnatal growth can be divided into phases that prioritize growth of different tissues beginning with vital organs, bone, muscle, and then adipose tissue. Muscle hypertrophy makes up the bulk of an animal's growth (Mohammadabadi et al., 2021), and as such, is the focus of our investigation. Additionally, the metabolic profile of skeletal muscle influences an animal's efficiency of nutrient utilization, and thus has implications on FE (Bottje et al., 2002; Kolath et al., 2006; Fu et al., 2017). Therefore, a growth model was used to evaluate changes in skeletal muscle metabolism from weaning to market. Ages were selected based on the completion of each phase diet fed at the Kansas State University Swine Unit, and pigs were harvested prior to moving on to the next phase of feeding. These phases are characterized by the essential nutrients a pig needs during that period of growth. For example, pigs are fed high quality amino acids to support high energy demands after weaning until 53 d, which are then reduced between 53 d and 87 d. Pigs are then moved to the finishing barn where diets are supplemented with carbohydrates, which are further increased at 120 d to meet high energy demands during finishing to reach market weight. Within each age group, three muscles with different inherent metabolic profiles were assessed to determine if underlying metabolic characteristics influence nutrient allocation and utilization in a growing animal. To evaluate muscle and adipose tissue growth at each age point, muscle cross sectional area (CSA) and BF thickness were measured.

Body weights, BF thickness, and muscle CSA were measured to evaluate muscle hypertrophy and fat growth at each age point. Our data showed a gradual increase in BW between 20 and 87 d, followed by a rapid increase in BW from 87 to 180 d (Figure 1A; $P < 0.01$). Similarly, BF thickness increased 2-fold from 120 to 180 d (Figure 1B; $P < 0.01$), which indicates a period of intensive adipose tissue growth. Cross sectional area was assessed to determine fiber size at

each age. Fibers in LD and LAT muscles increased at each age point after 53 d, while MS increased after 120 d (Figure 1C; $P < 0.01$). Of note, MS fiber size appears to stall between 87 and 120 d and 120 and 180 d, which is a period of rapid hypertrophy in LAT and LD muscle (Figure 1C; $P < 0.01$). This may be attributed to smaller fiber size in oxidative muscles compared to glycolytic muscles (Schiaffino and Reggiani, 2011) or location of the MS muscle in the body. Mitochondrial DNA (mtDNA) was assessed in the LD, LAT, and MS and used as an indicator of mitochondrial content to characterize metabolic changes that accompany muscle hypertrophy. Regardless of muscle, mtDNA copy number increased at 87 d compared to 20, 53, and 180 d and decreased from 87d to 180 d (Figure 1D; $P < 0.01$), which may indicate a period of metabolic remodeling that occurs at an age where hypertrophy is beginning to intensify. These data demonstrate intensive muscle hypertrophy begins at 53 d in LD and 87 d in LAT, while minimal hypertrophy occurs in MS. Additionally, 120 d marks the beginning of intensive adipose tissue growth.

Muscle allocates and uses nutrients in biochemical reactions that can aid in anabolic growth or be catabolized to meet energy demands. While both are necessary depending on cellular needs, the latter metabolizes intermediates in the TCA cycle and electron transport chain to produce ATP, heat, and CO_2, which represents a net loss of carbon that could otherwise be used for anabolic reactions that support muscle growth (Kong and Adeola, 2014). Glycolysis has the potential to conserve these carbon backbones. For example, glycolytic intermediates can branch into the pentose phosphate pathway (PPP) to generate 5-carbon precursors for nucleic acid and amino acid synthesis or the end product, pyruvate, can be recycled in the Cori cycle (Liu and Sabatini, 2020). To determine if growing muscle facilitates glycolytic intermediate allocation to the PPP, abundance of glucose-6-phosphate dehydrogenase (G6PDH) was assessed, which is a PPP entry point that converts glucose 6-phosphate to 6-phosphogluconolactone. Our results demonstrate the

abundance of G6PDH was lower at 87, 120, and 180 d in MS compared to LAT and LD (Figure 2A; $P < 0.01$), which suggests glycolytic muscles have a greater reliance on this anabolic pathway than oxidative muscles at these time points. To investigate changes in pyruvate entering the Cori cycle, lactate dehydrogenase alpha (LDHα) was assessed. Abundance of LDHα decreased in MS compared to LAT and LD regardless of age (Figure 2C; $P < 0.01$), which is not surprising considering glycolytic muscles have a greater pyruvate flux through LDHα (Washington et al., 2004). Additionally, LDHα decreased from 20 to 87 d regardless of muscle (Figure 2D; $P < 0.01$), which may be attributed to muscles being more glycolytic at weaning from lactose in a milk based diet (Menegat et al., 2019). These data showed glycolytic muscles have a greater abundance of enzymes associated with anabolism than oxidative muscles.

To establish a more comprehensive understanding of how muscles allocate and utilize nutrients to support muscle hypertrophy, we implemented an *in vitro* stable isotope tracing model adapted from Matarneh et al. (2021) to uncover changes in pyruvate-derived TCA intermediate flux. After incubation of isolated mitochondria with [$^{13}C_3$]-pyruvate and unlabeled malate, isotopomer enrichment patterns of TCA intermediates were analyzed (Figure 4). Briefly, the number of labelled carbons (or ^{13}C) in TCA intermediates derived from [$^{13}C_3$]-pyruvate can be detected using GC-MS. The enrichment patterns depict the number of ^{13}C in each intermediate that originated from [$^{13}C_3$]-pyruvate. Values for M + i represents the isotopomer proportions of a given metabolite, and therefore do not provide information on the total amount of metabolites in each sample but rather the contribution of pyruvate to the TCA cycle. For example, M + 2 citate is indicative of two ^{13}C in the citrate molecule originating from the labelled pyruvate molecule (Figure 4). These data, in combination with enzyme abundance of several oxidative enzymes,

provides a unique perspective on the metabolic adaptations that take place in muscle of a growing animal.

Pyruvate is an intermediate with multiple fates that can feed into the Cori cycle, as mentioned previously, or enter the TCA cycle through pyruvate dehydrogenase (PDH) or pyruvate carboxylase (PC). When pyruvate is converted to acetyl-CoA by PDH, CO_2 is produced and represents a loss of carbon to the animal. In the *in vitro* tracing model, an increase in M + 2 citrate suggests an increase in pyruvate entering the TCA cycle through PDH (Inigo et al., 2021). When unlabeled oxaloacetate combines with M + 2 acetyl-CoA, which is derived from PDH, M + 2 citrate is produced (Figure 4, black circles). On the other hand, PC converts pyruvate to oxaloacetate and consumes HCO_3^-, which produces M + 3 oxaloacetate in the tracing model (Figure 4, grey circles). In fact, PC abundance is higher in high-FE pigs than low-FE pigs (Fu et al., 2017), which depicts this anaplerotic enzyme as playing an important role in conserving carbons during carbohydrate oxidation. These labelling patterns can be traced throughout subsequent TCA reactions (Inigo et al., 2021), which are depicted theoretically as black or grey circles in Figure 4.

Enrichment fractions of oxaloacetate, citrate, alpha ketoglutarate, and succinate are reported. Our results show an increase in M2 (Figure 5D; $P < 0.05$) and M4 (Figure 5F; $P < 0.05$) citrate in LAT and MS mitochondria at 87 d compared to LD mitochondria. Regardless of muscle, citrate M3 increased at 87 d compared to 20, 53, and 120 d, while 180 d is intermediate (Figure 5E; $P < 0.01$). These data suggest at 87 d LD mitochondria may have a greater reliance on pyruvate entry into the TCA cycle through PC. Although no differences in PDH were found in LD at 87 d (Figure 3A; $P < 0.05$), activity of PDH is regulated by phosphorylation through pyruvate dehydrogenase kinase 4 (Kiilerich et al., 2010), which has not been measured at this time.

However, PDH abundance increased in MS at 53 and 180 d and increased at 120 d compared to 53 and 180 d (Figure 3A; $P < 0.05$). Further, abundance of PC did not increase at 87 d, and in fact, was greatest at 53 d (Figure 3D; $P < 0.01$) and corresponds to an increase in PDH at this age point compared to 53 d in LD and LAT mitochondria (Figure 3A; $P < 0.05$). Although isotopomer labeling patterns are indicative of enzymatic changes that would facilitate changes in intermediate use, the complex interplay between regulation of enzyme expression and activity increases the burden of elucidating these molecular mechanisms.

Further, M2, M3, and M4 citrate decreased between 87 and 120 d in all mitochondria (Figure 5D-F; $P < 0.05$), which corresponds to an increase in citrate synthase (CS) at 120 d (Figure 3G; $P < 0.01$). Additionally, abundance of CS was highest in MS compared to LD and LAT (Figure 3F; $P < 0.01$). These data suggest an increase in citrate production at this age, but the decrease in labelled citrate indicates citrate may be derived from other unlabeled metabolites or pyruvate-derived citrate is exiting the TCA cycle at this time. However, oxaloacetate M2, M3, and M4 increased in LD and LAT mitochondria at 120 d (Figure 5A-C; $P < 0.01$), which suggests the latter. Additionally, alpha-ketoglutarate M2 (Figure 6A; $P < 0.01$) and M3 (Figure 6B; $P < 0.01$) increased in LD and LAT compared to MS at 180 d, while alpha-ketoglutarate M4 increased in LD compared to MS at 180 d (Figure 6C; $P < 0.01$). Succinate M2 (Figure 6D; $P < 0.01$), M3 (Figure 6E; $P < 0.01$), and M4 (Figure 6F; $P < 0.01$) increased at 87 d, 120 d, and 180 d regardless of muscle. These data suggest pyruvate-derived citrate may be exiting the TCA cycle. In fact, citrate export from mitochondria is a source of cytosolic acetyl-CoA, which can be used for fatty acid synthesis or a precursor for histone acetylation. Since 120 d marks the beginning of an intensive period of adipose tissue growth, this represents a potential pathway that warrants further investigation as it may play a role in regulating nutrient partitioning.

Additionally, our findings showed an increase in M2 and M3 alpha-ketoglutarate at 180 d in LD and LAT mitochondria compared to MS (Figure 6A-B; $P < 0.01$). Interestingly, M2, M3, and M4 succinate increased at 87, 120, and 180 d regardless of muscle (Figure 6D-F; $P < 0.1$). These data suggest a loss of labeled carbon in LD and LAT mitochondria before alpha-ketoglutarate is converted to succinate. To determine if a subset of alpha-ketoglutarate is exiting the TCA cycle, we investigated the abundance of glutamate dehydrogenase (GDH), which showed an increase in LD compared to MS (Figure 7A; $P < 0.01$) and decrease at 137 d compared to 20 and 197 d (Figure 7B; $P < 0.05$). These data suggest alpha ketoglutarate exits the TCA cycle in glycolytic muscles presumably through GDH at 180 d. In fact, Hou and Wu (2018) reported L-glutamate is an important amino acid to maintain muscle growth in market weight swine, and as such is supplemented in finishing diets. Further, to investigate other enzymes that are involved in amino acid metabolism, abundance of glutamic-oxaloacetic transaminase 2 (GOT2) was assessed, which converts oxaloacetate to aspartate. Abundance of GOT2 increased in MS compared to LD (Figure 7D; $P < 0.01$) and increased at 120 d compared to 20 d in all muscles but was not different between 87 and 120 d (Figure 7E; $P < 0.01$), which may be attributed to the minimal muscle hypertrophy at weaning. These findings establish a foundation to investigate metabolic signaling that facilitate skeletal muscle hypertrophy; however, additional research is needed to uncover these mechanisms.

Conclusion

Our findings reveal changes in skeletal muscle metabolism that are accompanied by maturation. Our results indicate muscles characterized by glycolytic metabolism have a greater reliance on the PPP, which branches off glycolysis and supports muscle growth. Additionally, pyruvate entry and use within the TCA cycle varies at different age points and supports the notion

that muscle adjusts its metabolic characteristics to support different phases of muscle hypertrophy. Our findings also illustrate the complex dynamics between cataplerosis and anaplerosis of TCA intermediates, which have long been overlooked in muscle physiology of meat producing animals. In conclusion, these data depict the intricacies of muscle metabolism and highlight potential avenues in mitochondria metabolism that may be necessary for optimal nutrient utilization during lean deposition that warrant further investigation to improve FE in the swine industry.

References

Amirouche, A., A. C. Durieux, S. Banzet, N. Koulmann, R. Bonnefoy, C. Mouret, X. Bigard, A. Peinnequin, and D. Freyssenet. 2009. Down-regulation of Akt/mammalian target of rapamycin signaling pathway in response to myostatin overexpression in skeletal muscle. Endocrinology 150(1):286-294. doi: 10.1210/en.2008-0959

Andretta, I., F. M. W. Hickmann, A. Remus, C. H. Franceschi, A. B. Mariani, C. Orso, M. Kipper, M. P. Letourneau-Montminy, and C. Pomar. 2021. Environmental Impacts of Pig and Poultry Production: Insights From a Systematic Review. Front Vet Sci 8:750733. doi: 10.3389/fvets.2021.750733

Balaban, R. S. 1990. Regulation of oxidative phosphorylation in the mammalian cell. Am J Physiol 258(3 Pt 1):C377-389. doi: 10.1152/ajpcell.1990.258.3.C377

Bergmeyer, H. U. 1984. Methods of Enzymatic Analysis, Methods of Enzymatic Analysis, Verlag Chemie, Weinheim. p. 883-889.

Bikker, P., M. W. Verstegen, and M. W. Bosch. 1994. Amino acid composition of growing pigs is affected by protein and energy intake. J Nutr 124(10):1961-1969. doi: 10.1093/jn/124.10.1961

Bottje, W., M. Iqbal, Z. X. Tang, D. Cawthon, R. Okimoto, T. Wing, and M. Cooper. 2002. Association of mitochondrial function with feed efficiency within a single genetic line of male broilers. Poult Sci 81(4):546-555. doi: 10.1093/ps/81.4.546

Buzala, M., B. Janicki, and R. Czarnecki. 2015. Consequences of different growth rates in broiler breeder and layer hens on embryogenesis, metabolism and metabolic rate: A review. Poult Sci 94(4):728-733. doi: 10.3382/ps/pev015

Carnac, G., B. Vernus, and A. Bonnieu. 2007. Myostatin in the pathophysiology of skeletal muscle. Curr Genomics 8(7):415-422. doi: 10.2174/138920207783591672

Christoffolete, M. A., W. J. Silva, G. V. Ramos, M. R. Bento, M. O. Costa, M. O. Ribeiro, M. M. Okamoto, T. H. Lohmann, U. F. Machado, A. Musaro, and A. S. Moriscot. 2015. Muscle IGF-1-induced skeletal muscle hypertrophy evokes higher insulin sensitivity and carbohydrate use as preferential energy substrate. Biomed Res Int 2015:282984. doi: 10.1155/2015/282984

Cline, P. M., T. C. Tsai, C. A. Lents, A. M. Stelzleni, C. R. Dove, and M. Azain. 2022. Interaction of dietary carbohydrate and fat on glucose metabolism in growing pigs. Domest Anim Endocrinol 78:106655. doi: 10.1016/j.domaniend.2021.106655

Costa-Lima, B. R., S. P. Suman, S. Li, C. M. Beach, T. J. Silva, E. T. Silveira, B. M. Bohrer, and D. D. Boler. 2015. Dietary ractopamine influences sarcoplasmic proteome profile of pork Longissimus thoracis. Meat Sci 103:7-12. doi: 10.1016/j.meatsci.2014.12.008

Council, N. R. 2012. Nutrient Requirments of Swine. Eleventh Revised Edition ed. The National Academies Press, Washington DC.

Cruzat, V. F., and J. Tirapegul. 2015. Glutamine in Clinical Nutrition. Springer.

de Lange, P., M. Moreno, E. Silvestri, A. Lombardi, F. Goglia, and A. Lanni. 2007. Fuel economy in food-deprived skeletal muscle: signaling pathways and regulatory mechanisms. FASEB J 21(13):3431-3441. doi: 10.1096/fj.07-8527rev

Depreux, F. F., A. L. Grant, D. B. Anderson, and D. E. Gerrard. 2002. Paylean alters myosin heavy chain isoform content in pig muscle. J Anim Sci 80(7):1888-1894. doi: 10.2527/2002.8071888x

El-Kadi, S. W., R. L. t. Baldwin, K. R. McLeod, N. E. Sunny, and B. J. Bequette. 2009. Glutamate is the major anaplerotic substrate in the tricarboxylic acid cycle of isolated rumen epithelial and duodenal mucosal cells from beef cattle. J Nutr 139(5):869-875. doi: 10.3945/jn.108.103226

England, E. M., S. K. Matarneh, T. L. Scheffler, C. Wachet, and D. E. Gerrard. 2014. pH inactivation of phosphofructokinase arrests postmortem glycolysis. Meat Sci 98(4):850-857. doi: 10.1016/j.meatsci.2014.07.019

Frazier, A. E., Thorburn, David R. 2011. Biochemical Analyses of the Electron Transport Chain Complexes by Spectrophotometry, Mitochondrial Disorders No. 837. p. 49-62.

Frontera, W. R., and J. Ochala. 2015. Skeletal muscle: a brief review of structure and function. Calcif Tissue Int 96(3):183-195. doi: 10.1007/s00223-014-9915-y

Fu, L., Y. Xu, Y. Hou, X. Qi, L. Zhou, H. Liu, Y. Luan, L. Jing, Y. Miao, S. Zhao, H. Liu, and X. Li. 2017. Proteomic analysis indicates that mitochondrial energy metabolism in skeletal muscle tissue is negatively correlated with feed efficiency in pigs. Sci Rep 7:45291. doi: 10.1038/srep45291

Gerrard, D., and A. Grant. 2003. Principles of Animal Growth and Development. Kendall/Hunt Publishing Company.

Glass, D. J. 2005. Skeletal muscle hypertrophy and atrophy signaling pathways. Int J Biochem Cell Biol 37(10):1974-1984. doi: 10.1016/j.biocel.2005.04.018

Gondret, F., N. Le Floc'h, D. I. Batonon-Alavo, M. H. Perruchot, Y. Mercier, and B. Lebret. 2021. Flash dietary methionine supply over growth requirements in pigs: Multi-facetted effects on skeletal muscle metabolism. Animal 15(7):100268. doi: 10.1016/j.animal.2021.100268

Gravel, S. P., S. Andrzejewski, D. Avizonis, and J. St-Pierre. 2014. Stable isotope tracer analysis in isolated mitochondria from mammalian systems. Metabolites 4(2):166-183. doi: 10.3390/metabo4020166

Gunawan, A. M., B. T. Richert, A. P. Schinckel, A. L. Grant, and D. E. Gerrard. 2007. Ractopamine induces differential gene expression in porcine skeletal muscles. J Anim Sci 85(9):2115-2124. doi: 10.2527/jas.2006-540

Gunawan, A. M., C. N. Yen, B. T. Richert, A. P. Schinckel, A. L. Grant, and D. E. Gerrard. 2020. Ractopamine-induced fiber type-specific gene expression in porcine skeletal muscles is independent of growth. J Anim Sci 98(11)doi: 10.1093/jas/skaa341

Guo, X., Zhang, W., Li, M., Gao, P., He, Z., Wu, Y., Cai, C., Li, B., Cao., G. 2019. Transcriptome profile of skeletal muscle at different developmental stages in Large White and Mashen pigs. Canadian Journal of Animal Science 99doi: https://doi.org/10.1139/cjas-2019-0002

Halsey, C. H., P. S. Weber, S. S. Reiter, B. N. Stronach, J. L. Bartosh, and W. G. Bergen. 2011. The effect of ractopamine hydrochloride on gene expression in adipose tissues of finishing pigs. J Anim Sci 89(4):1011-1019. doi: 10.2527/jas.2010-3269

Hinson, R. B., B. R. Wiegand, M. J. Ritter, G. L. Allee, and S. N. Carr. 2011. Impact of dietary energy level and ractopamine on growth performance, carcass characteristics, and meat quality of finishing pigs. J Anim Sci 89(11):3572-3579. doi: 10.2527/jas.2010-3302

Hou, Y., and G. Wu. 2018. L-Glutamate nutrition and metabolism in swine. Amino Acids 50(11):1497-1510. doi: 10.1007/s00726-018-2634-3

Inigo, M., S. Deja, and S. C. Burgess. 2021. Ins and Outs of the TCA Cycle: The Central Role of Anaplerosis. Annu Rev Nutr 41:19-47. doi: 10.1146/annurev-nutr-120420-025558

James, B. W., M. D. Tokach, R. D. Goodband, J. L. Nelssen, S. S. Dritz, K. Q. Owen, J. C. Woodworth, and R. C. Sulabo. 2013a. Effects of dietary L-carnitine and ractopamine HCl

on the metabolic response to handling in finishing pigs. J Anim Sci 91(9):4426-4439. doi: 10.2527/jas.2011-4411

James, B. W., M. D. Tokach, R. D. Goodband, J. L. Nelssen, S. S. Dritz, K. Q. Owen, J. C. Woodworth, and R. C. Sulabo. 2013b. Interactive effects of dietary ractopamine HCl and L-carnitine on finishing pigs: I. Growth performance. J Anim Sci 91(7):3265-3271. doi: 10.2527/jas.2011-4286

Jastroch, M., A. S. Divakaruni, S. Mookerjee, J. R. Treberg, and M. D. Brand. 2010. Mitochondrial proton and electron leaks. Essays Biochem 47:53-67. doi: 10.1042/bse0470053

Julien, I. B., C. F. Sephton, and P. A. Dutchak. 2018. Metabolic Networks Influencing Skeletal Muscle Fiber Composition. Frontiers in Cell and Developmental Biology (125)doi: 10.3389/fcell.2018.00125

Khanal, P., C. Maltecca, C. Schwab, K. Gray, and F. Tiezzi. 2019. Genetic parameters of meat quality, carcass composition, and growth traits in commercial swine. J Anim Sci 97(9):3669-3683. doi: 10.1093/jas/skz247

Kiilerich, K., H. Adser, A. H. Jakobsen, P. A. Pedersen, D. G. Hardie, J. F. Wojtaszewski, and H. Pilegaard. 2010. PGC-1alpha increases PDH content but does not change acute PDH regulation in mouse skeletal muscle. Am J Physiol Regul Integr Comp Physiol 299(5):R1350-1359. doi: 10.1152/ajpregu.00400.2010

Kolath, W. H., M. S. Kerley, J. W. Golden, and D. H. Keisler. 2006. The relationship between mitochondrial function and residual feed intake in Angus steers. J Anim Sci 84(4):861-865. doi: 10.2527/2006.844861x

Komarek, A. M., S. Dunston, D. Enahoro, H. C. J. Godfray, M. Herrero, D. Mason-D'Croz, K. M. Rich, P. Scarborough, M. Springmann, T. B. Sulser, K. Wiebe, and D. Willenbockel. 2021. Income, consumer preferences, and the future of livestock-derived food demand. Glob Environ Change 70:102343. doi: 10.1016/j.gloenvcha.2021.102343

Kong, C., and O. Adeola. 2014. Evaluation of amino Acid and energy utilization in feedstuff for Swine and poultry diets. Asian-Australas J Anim Sci 27(7):917-925. doi: 10.5713/ajas.2014.r.02

Lipina, C., H. Kendall, A. C. McPherron, P. M. Taylor, and H. S. Hundal. 2010. Mechanisms involved in the enhancement of mammalian target of rapamycin signalling and hypertrophy in skeletal muscle of myostatin-deficient mice. FEBS Lett 584(11):2403-2408. doi: 10.1016/j.febslet.2010.04.039

Liu, G. Y., and D. M. Sabatini. 2020. mTOR at the nexus of nutrition, growth, ageing and disease. Nat Rev Mol Cell Biol 21(4):183-203. doi: 10.1038/s41580-019-0199-y

Lopez-Andreo, M., L. Lugo, A. Garrido-Pertierra, M. I. Prieto, and A. Puyet. 2005. Identification and quantitation of species in complex DNA mixtures by real-time polymerase chain reaction. Anal Biochem 339(1):73-82. doi: 10.1016/j.ab.2004.11.045

Main, R., S. S. Dritz, M. D. Tokach, R. D. Goodband, J. L. Nelssen, and J. M. DeRouchey. 2009. Effects of ractopamine HCl dose and treatment period on pig performance in a commercial finishing facility. Journal of Swine Health and Production 17(3):134-139.

Martinez-Reyes, I., and N. S. Chandel. 2020. Mitochondrial TCA cycle metabolites control physiology and disease. Nat Commun 11(1):102. doi: 10.1038/s41467-019-13668-3

Matarneh, S. K., C. N. Yen, J. Bodmer, S. W. El-Kadi, and D. E. Gerrard. 2021. Mitochondria influence glycolytic and tricarboxylic acid cycle metabolism under postmortem simulating conditions. Meat Sci 172:108316. doi: 10.1016/j.meatsci.2020.108316

McBride, W. D., and N. Key. 2013. U.S. Hog Production From 1992 to 2009: Technology, Restructuring, and Productivity Growth. USDA Economic Research Service

Menegat, M. B., R. D. Goodband, J. M. DeRouchey, M. D. Tokach, J. C. Woodworth, and S. S. Dritz. 2019. Kansas State University Swine Nutrition Guide: *Nursery Phase Feeding Program*.

Merz, K. E., and D. C. Thurmond. 2021. Role of Skeletal Muscle in Insulin Resistance and Glucose Uptake. Comparative Physiology 10(3)doi: 10.1002/cphy.c190029

Mishra, P., G. Varuzhanyan, A. H. Pham, and D. C. Chan. 2015. Mitochondrial Dynamics is a Distinguishing Feature of Skeletal Muscle Fiber Types and Regulates Organellar Compartmentalization. Cell Metab 22(6):1033-1044. doi: 10.1016/j.cmet.2015.09.027

Mohammadabadi, M., F. Bordbar, J. Jensen, M. Du, and W. Guo. 2021. Key Genes Regulating Skeletal Muscle Development and Growth in Farm Animals. Animals (Basel) 11(3)doi: 10.3390/ani11030835

Montelli, N., T. Alvarenga, A. K. Almeida, F. A. P. Alvarenga, I. F. Furusho-Garcia, P. L. Greenwood, and I. G. Pereira. 2021. Associations of feed efficiency with circulating IGF-1 and leptin, carcass traits and meat quality of lambs. Meat Sci 173:108379. doi: 10.1016/j.meatsci.2020.108379

Mouisel, E., K. Relizani, L. Mille-Hamard, R. Denis, C. Hourde, O. Agbulut, K. Patel, L. Arandel, S. Morales-Gonzalez, A. Vignaud, L. Garcia, A. Ferry, S. Luquet, V. Billat, R. Ventura-Clapier, M. Schuelke, and H. Amthor. 2014. Myostatin is a key mediator between energy metabolism and endurance capacity of skeletal muscle. Am J Physiol Regul Integr Comp Physiol 307(4):R444-454. doi: 10.1152/ajpregu.00377.2013

Niyas, A., C. K, S. S, S. V, B. R, B. M, Rao, Kurien, and Girish. 2015. Adaptation of Livestock to Environmental Challenges. Veterinary Science and Medical Diagnosis 4doi: 10.4172/2325-9590.1000146

Patience, J. F., M. C. Rossoni-Serao, and N. A. Gutierrez. 2015. A review of feed efficiency in swine: biology and application. J Anim Sci Biotechnol 6(1):33. doi: 10.1186/s40104-015-0031-2

Picard, B., L. Lefaucheur, C. Berri, and M. J. Duclos. 2002. Muscle fibre ontogenesis in farm animal species. Reprod Nutr Dev 42(5):415-431. doi: 10.1051/rnd:2002035

Plaitakis, A., E. Kalef-Ezra, D. Kotzamani, I. Zaganas, and C. Spanaki. 2017. The Glutamate Dehydrogenase Pathway and Its Roles in Cell and Tissue Biology in Health and Disease. Biology (Basel) 6(1)doi: 10.3390/biology6010011

Risson, V., L. Mazelin, M. Roceri, H. Sanchez, V. Moncollin, C. Corneloup, H. Richard-Bulteau, A. Vignaud, D. Baas, A. Defour, D. Freyssenet, J. F. Tanti, Y. Le-Marchand-Brustel, B. Ferrier, A. Conjard-Duplany, K. Romanino, S. Bauche, D. Hantai, M. Mueller, S. C. Kozma, G. Thomas, M. A. Ruegg, A. Ferry, M. Pende, X. Bigard, N. Koulmann, L. Schaeffer, and Y. G. Gangloff. 2009. Muscle inactivation of mTOR causes metabolic and dystrophin defects leading to severe myopathy. J Cell Biol 187(6):859-874. doi: 10.1083/jcb.200903131

Scheffler, T. L., J. M. Scheffler, S. Park, S. C. Kasten, Y. Wu, R. P. McMillan, M. W. Hulver, M. I. Frisard, and D. E. Gerrard. 2014. Fiber hypertrophy and increased oxidative capacity can occur simultaneously in pig glycolytic skeletal muscle. Am J Physiol Cell Physiol 306(4):C354-363. doi: 10.1152/ajpcell.00002.2013

Schiaffino, S., and C. Reggiani. 2011. Fiber types in mammalian skeletal muscles. Physiol Rev 91(4):1447-1531. doi: 10.1152/physrev.00031.2010

Schumacher, M., H. DelCurto-Wyffels, J. Thomson, and J. Boles. 2022. Fat Deposition and Fat Effects on Meat Quality-A Review. Animals (Basel) 12(12)doi: 10.3390/ani12121550

Shi, L., and B. P. Tu. 2015. Acetyl-CoA and the regulation of metabolism: mechanisms and consequences. Curr Opin Cell Biol 33:125-131. doi: 10.1016/j.ceb.2015.02.003

Stitt, T. N., D. Drujan, B. A. Clarke, F. Panaro, Y. Timofeyva, W. O. Kline, M. Gonzalez, G. D. Yancopoulos, and D. J. Glass. 2004. The IGF-1/PI3K/Akt pathway prevents expression of muscle atrophy-induced ubiquitin ligases by inhibiting FOXO transcription factors. Mol Cell 14(3):395-403. doi: 10.1016/s1097-2765(04)00211-4

Tabassum, N., Kheya, Ilora Shabnam, Asaduzzaman, Syed Abdullah Ibn, Maniha, Syeda Muntaka, Fayz, Abrar Hamim, Zakaria, Amayna, Noor, Rashed. 2020. A Review on the Possible Leakage of Electrons through the Electron Transport Chain within Mitochondria. Biomedical Research and Environmental Sciences 1(4)doi: 10.37871/jels1127

Tokach, M. D., B. D. Goodband, and T. G. O'Quinn. 2016. Performance-enhancing technologies in swine production. Animal Frontiers 6(4)doi: doi.org/10.2527/af.2016-0039

Tripathi, A. D., Mishra, Richa, Maurya, Kamlesh K., Singh, Ram B., Wilson, Douglas W. 2019. Estimates for World Population and Global Food Availability for Global Health. In: R. B. Singg, Watson, Ronald Ross, Takahashi, Toru, editor, The Role of Functional Food Security in Global Health. p. 3-24.

Wagner, J. R., A. P. Schinckel, W. Chen, J. C. Forrest, and B. L. Coe. 1999. Analysis of body composition changes of swine during growth and development. J Anim Sci 77(6):1442-1466. doi: 10.2527/1999.7761442x

Washington, T. A., J. M. Reecy, R. W. Thompson, L. L. Lowe, J. M. McClung, and J. A. Carson. 2004. Lactate dehydrogenase expression at the onset of altered loading in rat soleus muscle. J Appl Physiol (1985) 97(4):1424-1430. doi: 10.1152/japplphysiol.00222.2004

White, B. A., J. R. Harrison, and L. M. Mehlmann. 2019. Energy Metabolism. Endocrine and Reproductive Physiology 3:40-76.

Williams, N. H., T. R. Cline, A. P. Schinckel, and D. J. Jones. 1994. The impact of ractopamine, energy intake, and dietary fat on finisher pig growth performance and carcass merit. J Anim Sci 72(12):3152-3162. doi: 10.2527/1994.72123152x

Wu, G., F. W. Bazer, G. A. Johnson, D. A. Knabe, R. C. Burghardt, T. E. Spencer, X. L. Li, and J. J. Wang. 2011. Triennial Growth Symposium: important roles for L-glutamine in swine nutrition and production. J Anim Sci 89(7):2017-2030. doi: 10.2527/jas.2010-3614

Zahid, H. J., E. Robinson, and R. L. Kelly. 2016. Agriculture, population growth, and statistical analysis of the radiocarbon record. Proc Natl Acad Sci U S A 113(4):931-935. doi: 10.1073/pnas.1517650112

Zhao, J., J. J. Brault, A. Schild, P. Cao, M. Sandri, S. Schiaffino, S. H. Lecker, and A. L. Goldberg. 2007. FoxO3 coordinately activates protein degradation by the autophagic/lysosomal and proteasomal pathways in atrophying muscle cells. Cell Metab 6(6):472-483. doi: 10.1016/j.cmet.2007.11.004

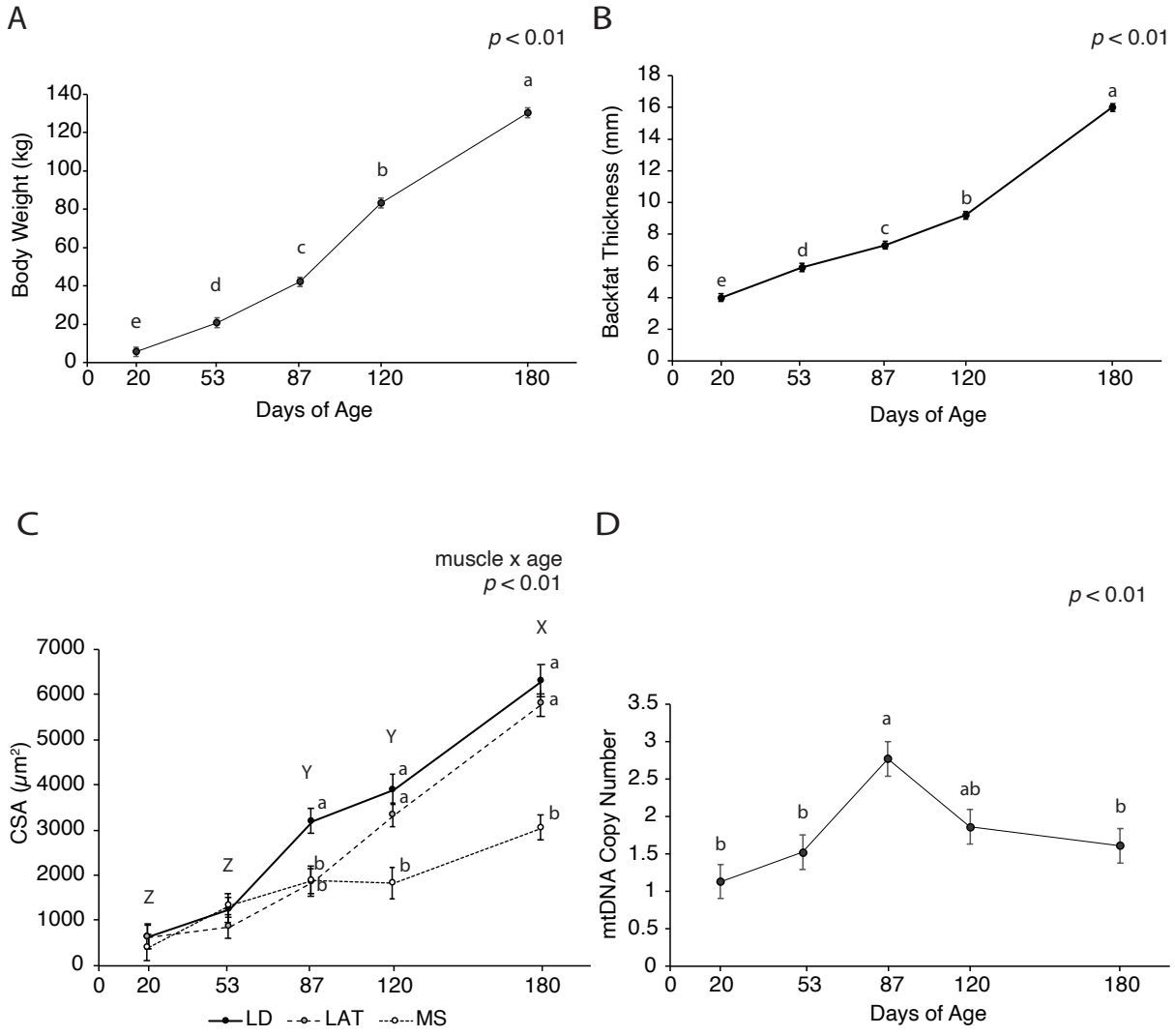

Figure 1. Growth characteristics of pigs at each age point. (A) Body weight (B) and backfat thickness of pigs at 20, 53, 87, 120, and 180 d. (C) Muscle cross sectional area (CSA) of LD, LAT, and LD muscles collected from pigs at each age point. (D) Muscle mitochondrial DNA (mtDNA) copy number at each age point. Data are means ± SE. Five barrows per age group (n = 5). Means lacking a common letter (a, b, c) differ within a time point ($p < 0.05$). X, Y, Z represent differences between ages.

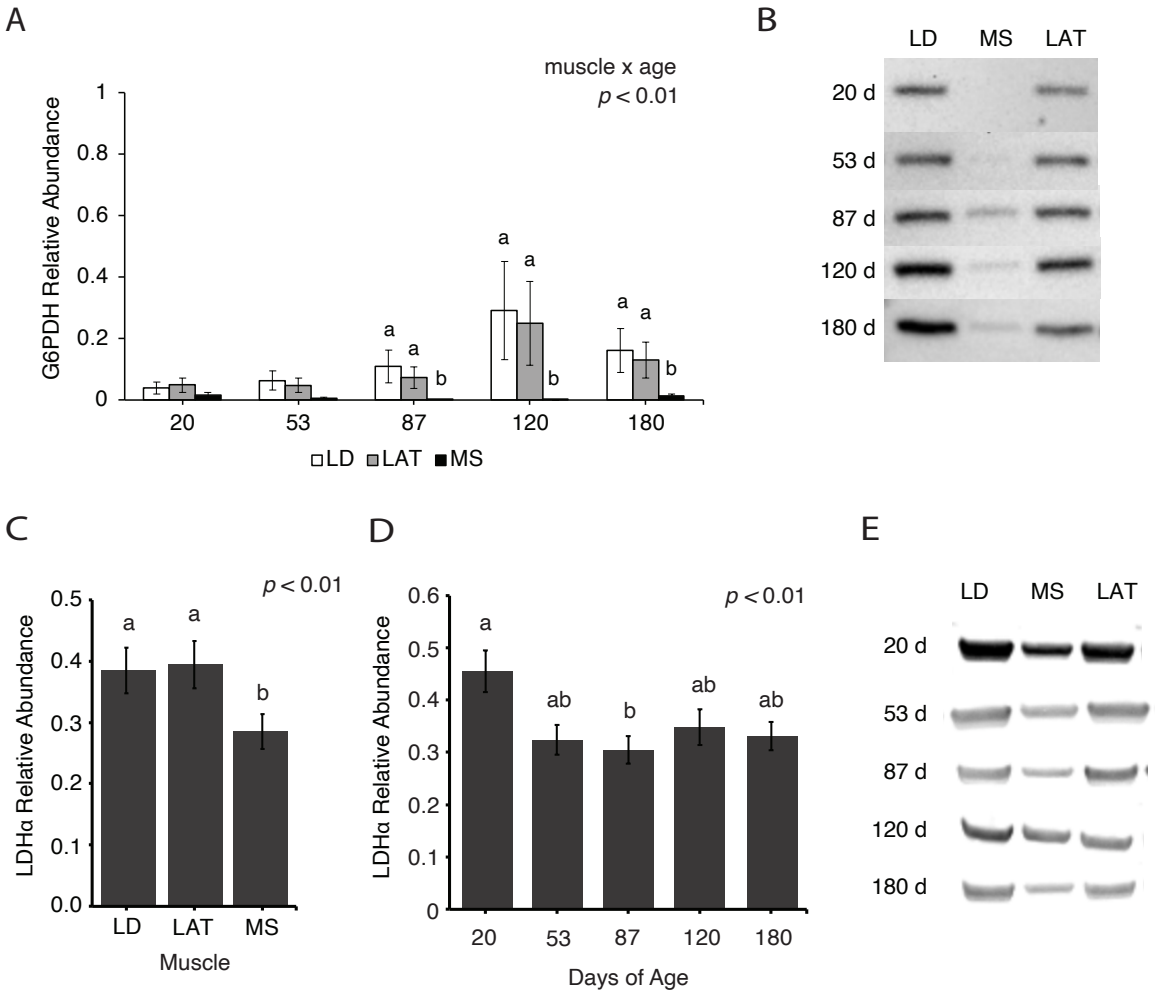

Figure 2. Relative abundance of glycolytic enzymes. **(A)** Relative abundance of glucose-6-phosphate dehydrogenase (G6PDH). **(B)** Representative images of Western blots quantified in (A). **(C-D)** Relative abundance of lactate dehydrogenase alpha (LDHα) in each (C) muscle and (D) age group. **(E)** Representative images of Western blots quantified in (C-D). Abundance of proteins of interest were normalized to total protein. Data are means ± SE. Five barrows per age group (n = 5). Means lacking a common letter differ within a time point ($p < 0.05$).

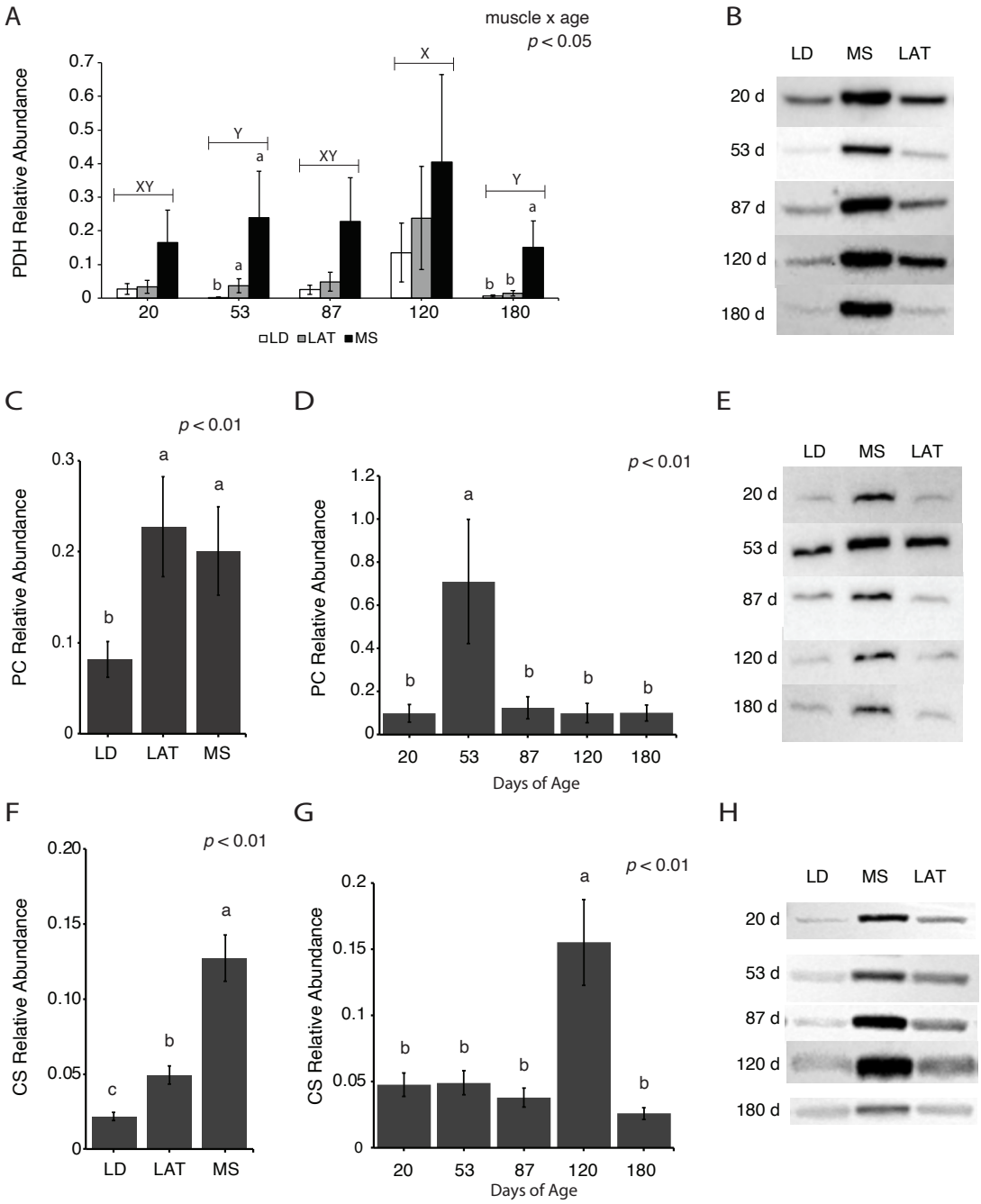

Figure 3. Relative abundance of several oxidative enzymes. **(A)** Relative abundance of pyruvate dehydrogenase (PDH). **(B)** Representative images of Western blots quantified in (A). **(C-D)** Relative abundance of pyruvate carboxylase (PC) in each (C) muscle and (D) age group. **(E)** Representative images of Western blots quantified in (C-D). **(F-G)** Relative abundance of citrate synthase (CS) in each (F) muscle and (G) age group. **(H)** Representative images of Western blots quantified in (F-G). Abundance of proteins of interest were normalized to total protein. Data are

means ± SE. Five barrows per age group (n = 5). Means lacking a common letter differ within a time point ($p < 0.05$).

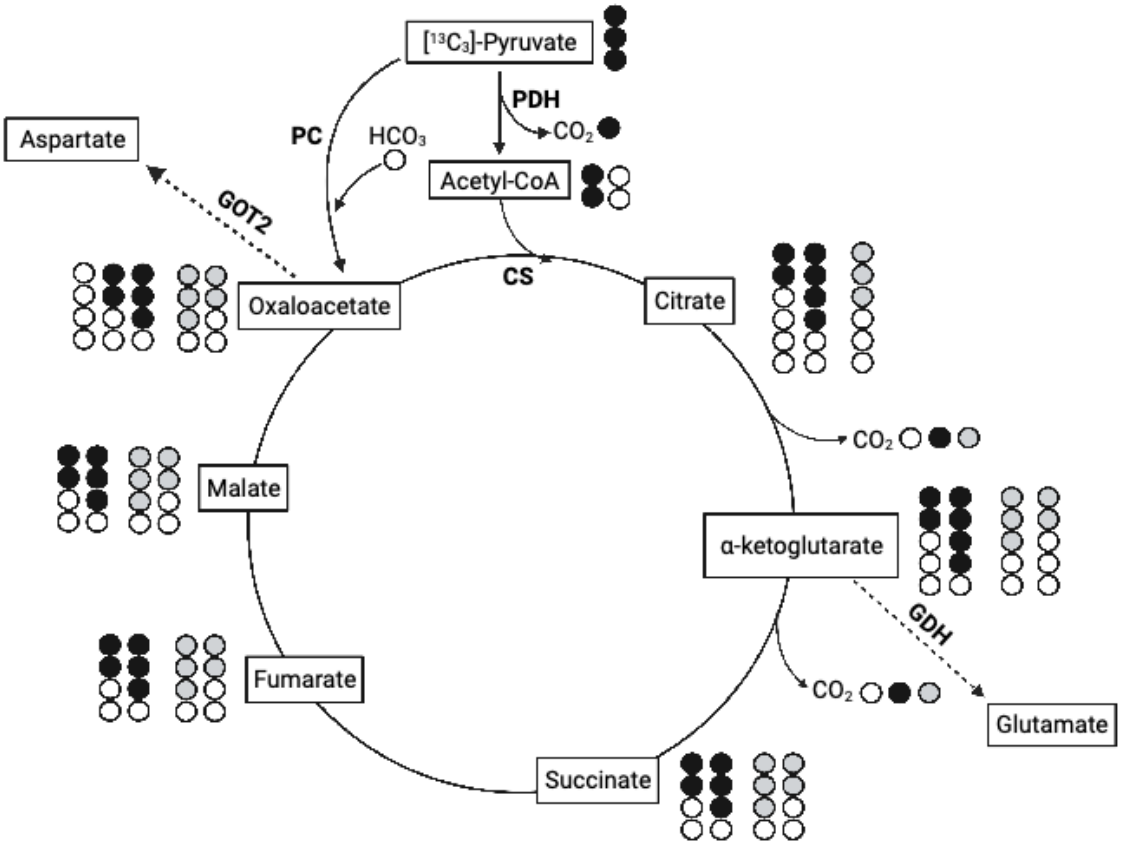

Figure 4. Schematic of theoretical labeling patterns of TCA intermediates after isolated mitochondria are incubated with [$^{13}C_3$]-pyruvate. Black circles are ^{13}C derived from [$^{13}C_3$]-pyruvate that enter the TCA cycle through pyruvate dehydrogenase (PDH). Grey circles indicate ^{13}C derived from [$^{13}C_3$]- pyruvate that enter the TCA cycle through pyruvate carboxylase (PC). White circles represent unlabeled carbon atoms (^{12}C). Dashed lines indicate enzymatic reactions involved in amino acid metabolism.

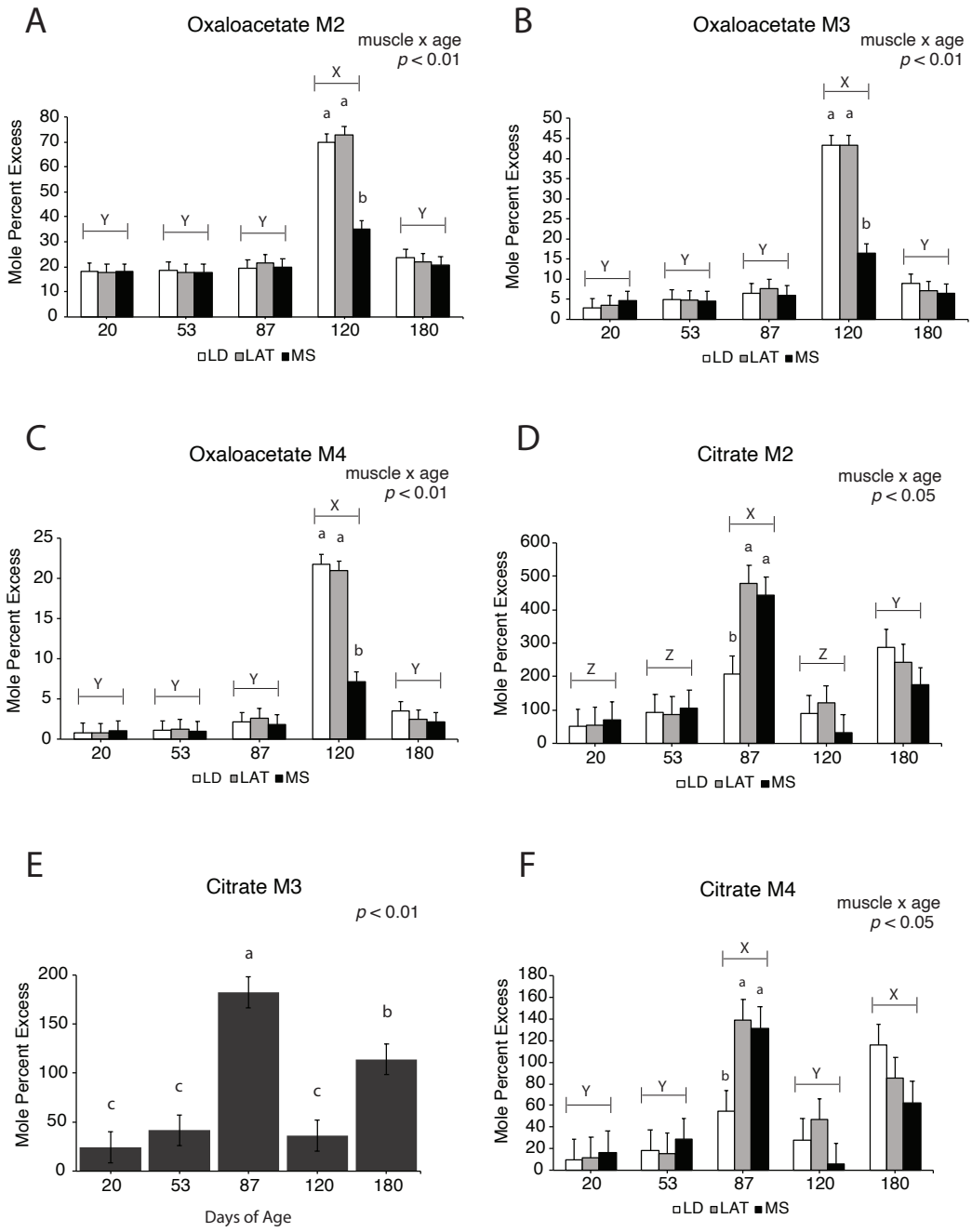

Figure 5. [$^{13}C_3$]-pyruvate derived isotopomer enrichments in isolated mitochondria. **(A-C)** Enrichment of (A) M2, (B), M3, and (C) M4 oxaloacetate in LD, LAT, and LD mitochondria isolated from pigs at each age point. **(D-F)** Enrichment of (A) M2, (B), M3, and (C) M4 citrate in LD, LAT, and LD mitochondria isolated from pigs at each age point. Data are means ± SE. Mitochondria were isolated from LD, LAT, and MS muscles of five barrows per age group (n=5).

Means lacking a common letter (a, b, c) differ within a time point ($p < 0.05$). X, Y, Z represent differences between ages.

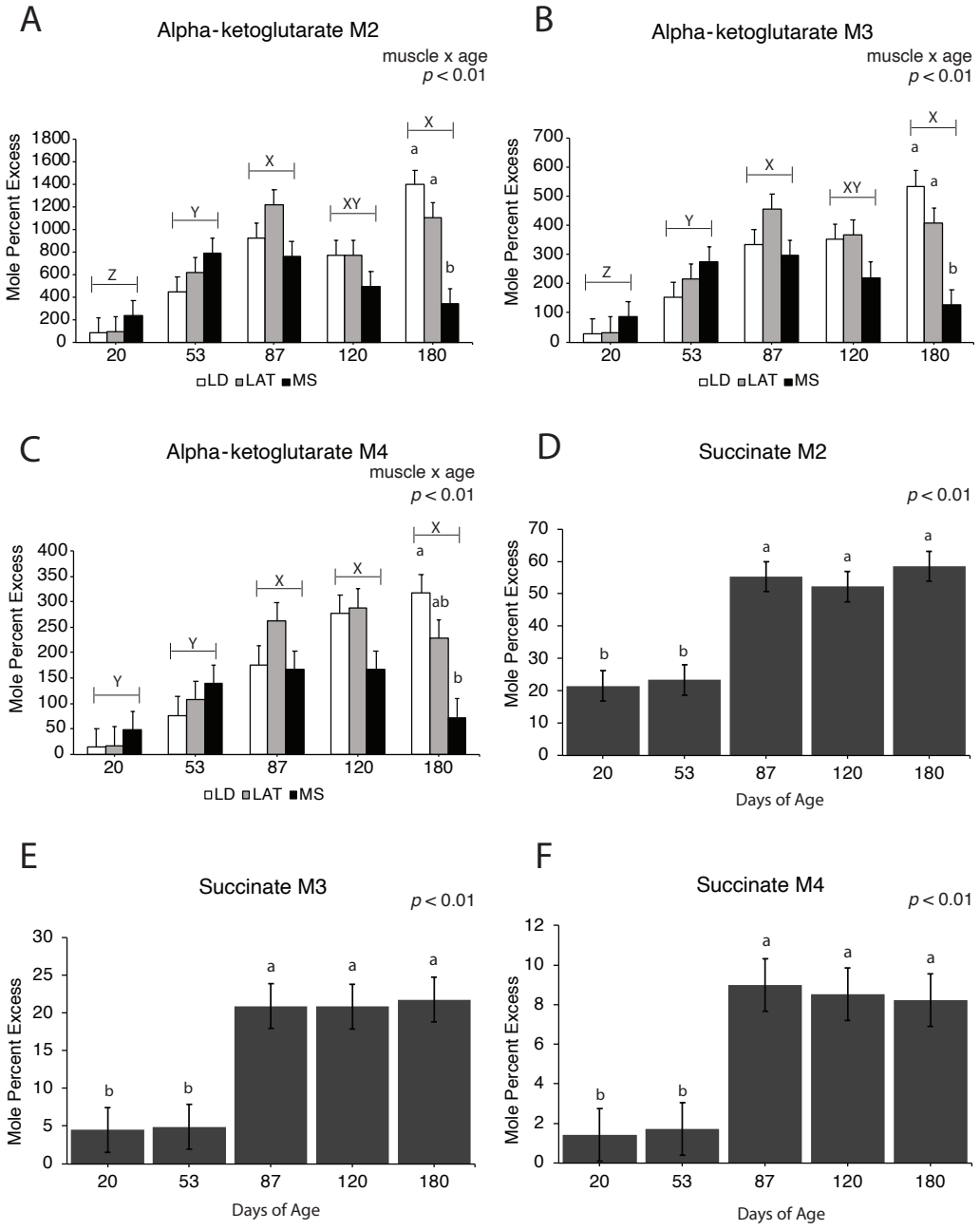

Figure 6. [$^{13}C_3$]-pyruvate derived isotopomer enrichments in isolated mitochondria. **(A-C)** Enrichment of (A) M2, (B), M3, and (C) M4 alpha ketoglutarate in LD, LAT, and LD mitochondria isolated from pigs at each age point. **(D-F)** Enrichment of (A) M2, (B), M3, and (C) M4 succinate in LD, LAT, and LD mitochondria isolated from pigs at each age point. Data are means ± SE.

Mitochondria were isolated from LD, LAT, and MS muscles of five barrows per age group (n=5). Means lacking a common letter (a, b, c) differ within a time point ($p < 0.05$). X, Y, Z represent differences between ages.

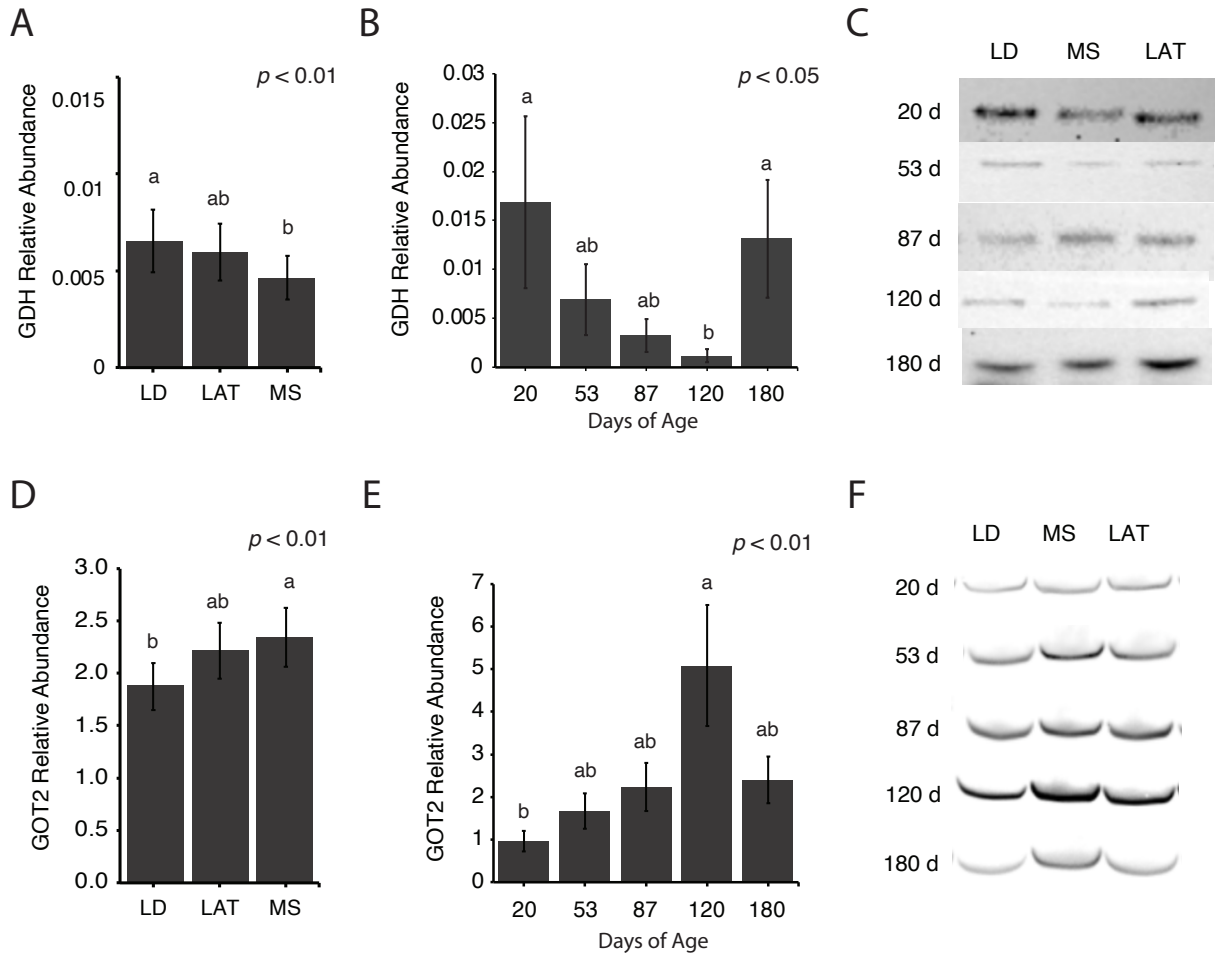

Figure 7. Relative abundance of enzymes involved in amino acid metabolism. **(A-B)** Relative abundance of glutamate dehydrogenase (GDH) in each (A) muscle and (B) age group. **(C)** Representative images of Western blots quantified in (A-B). **(D-E)** Relative abundance of glutamic-oxaloacetic transaminase (GOT2) in each (D) muscle and (E) age group. **(F)** Representative images of Western blots quantified in (D-E). Abundance of proteins of interest were normalized to total protein. Data are means ± SE. Five barrows per age group (n = 5). Means lacking a common letter differ within a time point ($p < 0.05$).